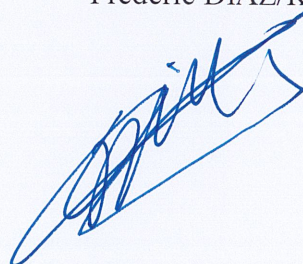Marseille, November 17, 2020

To the Editor,
Geoscientific Model Development

Please find enclosed the second revised version of our research article entitled *"Implementation and assessment of a carbonate system model (Eco3M-CarbOxv1.1) in a highly-dynamic Mediterranean coastal site (Bay of Marseille, France)"*. We considered all the valuable comments of the Dr. Munhoven and especially, we addressed the point on the poor scientific justification of the River intrusion experiment. We hope that our manuscript may now be accepted for final publication.
All authors approved the final version of the paper for submission.

Sincerely,

Frédéric DIAZ/Katixa LAJAUNIE-SALLA

Review of the first revised version of

"Implementation and assessment of a carbonate system model (Eco3M-CarbOxv1.1) in a highly-dynamic Mediterranean coastal site (Bay of Marseille, France)"

submitted for publication to Geoscientific Model Development
by K. Lajaunie-Salla and co-authors

General reply: We thank again the Reviewer Dr Munhoven for his second evaluation of our work. We thank too him for the detailed and useful comments that contributed to greatly improve the manuscript. We consider all of his comments to improve the manuscript.

1. General comments

The authors' reply the revised manuscript are not very "reviewer-friendly." It is nowadays standard practice to provide a "track change" (or a LATEXDIFF) version of the manuscript clearly identifying the changes made to the text, right in the text. The equivalent information is seemingly given in the reply, except that the line numbers provided there do not match, so that one has to search manually for the exact location of the changes.

The preparation of the manuscript would also have benefited from some extra care. Page numbers restart at 1 after page 23 without any apparent reason.

Reply : The preparation of the revised ms has been reviewed with care and page numbers have been reprocessed. A new check of the different sections has been carefully performed.

1.1 Appreciation of the replies to reviewers

The authors have all in all well responded to the referees' comments, with one exception though. In the response to my comment 2.3, regarding the missing effect of river intrusions on DIC — TA perturbations are taken into account, but as these are carried mainly by HCO_3^-, they also generate DIC perturbations of the same magnitude, which are neglected — I read at the top of the fourth page (page numbers in the response would have been helpful) that

"Concerning the riverine inputs scenarii, we decide to focus on nitrate and alkalinity supply. In fact the model simulates the DIC increases, as is observed, which highlight that the carbonate system module is well resolved."

The reply to the comments is somewhat ambiguous as suggests that DIC changes are taken into account, while they are actually not, as stated in the manuscript at lines 413–414 :

" [. . .] the experimental design on the Rhône River supply only considers the TA perturbation on the carbonate system but not that due to the DIC supply."

So, even if the model reproduces the observed DIC increases (as stated in the reply), this must obviously be for the wrong reasons, as only one half of the effects of the perturbation due to river intrusions is taken into account. By the way, no one argued that the carbonate system module was not well resolved.

Reply : We decided to remove the scenario of AT supply by river and all the text refered to it in the methods and results/discussion sections. See our detailed comment on this point hereafter.

1.2 Appreciation of the revised manuscript

The model description has been improved and the rationale behind the carbonate speciation calculations is now presented in a new appendix. Unfortunately, the layout of that appendix is rather chaotic which makes it difficult to read.

2. Specific comments
2.1 River intrusion experiments: poor justification
The justification added at lines 414–417 for taking the effect of river intrusions into account only in terms of the resulting TA but not DIC perturbations is rather cavalier and scientifically untenable. This is a completely unrealistic assumption that makes the outcome of the experiment meaningless and thus essentially invalidates any conclusion drawn from it.

I only see two options to address this shortcoming:
1. the river intrusion experiments are repeated with the effect on DIC included (which should be rather straightforward to correct) and the discussion of the results adapted;
2. these experiments are simply taken out of the paper as the current results are essentially unfounded.
Even in preliminary experiments, one must not chose to disregard one of two effects of a perturbation if these are of the same order of magnitude. Such arbitrary choices lead to arbitrary results.

Reply : We have chosen the second option proposed by the Reviewer. Mainly because it was not straightforward to consider DIC supply by River as considered for AT. In fact DIC is not as conservative as AT is regard to salinity. It is then impossible to use a relationship between DIC and salinity as that used between AT and salinity in the previous version of our manuscript. In the context of a 0D modelling developed here, this kind of relationship would have been the only mean to take into account the DIC supply by the Rhône River. In the revised version, we stressed (l 398-401) that rivers also supply TA and DIC and a consideration for these supplies in future works may sensibly modify the modeled carbonate balance in the BoM compared to that presented in this study. Concomitantly we slightly rewrote the end of section 4.1 on the model performance in Discussion.

As noted in the conclusion (l434), a coupling of the Eco3M-CarbOx model to a 3D hydrodynamics model is planed to better represent the complexity of functioning of the BOM. This implementation will enable, for example, to take into account actual DIC and AT supplies from the Rhône River by considering forcing values measured in the River.

3. Technical comments
Reply : All these technical comments have been taken into account in the new revised version of ms.

Page 1, line 22: "the year 2017 that is a period for which" should read "the year 2017 for which"
Page 1, line 25: "of most of variables of carbonate system except Total Alkalinity." should read "of most of the variables of the carbonate system except for Total Alkalinity."
Page 1, line 26: "experiments were also conducted" should read "experiments were conducted"
Page 1, line 26: "to (i) seawater" should read "to (i) a seawater"
Page 1, line 27: "Rhône River plume intrusion" should read "Rhône River plume intrusions"; by the way: the name of that river is sometimes spelled "Rhône", more often "Rhone" — please use the same spelling consistently throughout
Page 1, line 35: "external forcing have" should read "external forcings have"
Page 5, line 188: "a salinity threshold of 37 has been chosen" – is this correct? A threshold of 37 looks rather high to me.
Page 6, line 226: "during MWC period" should read "during the MWC period"
Page 7, line 271: "15 March and 6 May" should either read "15th March and 6th May" or "March 15th and May 6th" (as on line 277, p. 8)

Page 11, line 390: "Moreover, previous study" should read "Moreover, a previous study", or even better reformulate the sentence to read "Moreover, Fraysse et al. (2013) highlight that . . . " and discard the citation in brackets.

Page 11, line 402: "a longer period ca. 15 days" should read "a longer period of ca. 15 days"

Page 11, lines 402–403: "high atmospheric pCO2 value and wind speed" better had to read "high atmospheric pCO2 and high wind speeds"

Page 11, line 411: "due to some two" should read "due to two"

29th and 30th pages (pages nr. 6 and 7), throughout: "in the pH scale" should read "on the pH scale"

29th page (page nr. 6): "Concentration in Total Fluoride (TF) ions" should read "Total Fluoride concentration" (without "ions," as TF includes the non ionic HF)

29th page (page nr. 6): "Concentration in Total Sulphate (TS) ions" should read "Total Sulphate concentration" ("ions" is superfluous)

29th page (page nr. 6): "Concentration in Total Boron (TB)" should read "total boron concentration" (without "ions," as TB includes the non ionic B(OH)3)

29th page (page nr. 6): KF is the dissociation constant of hydrogen fluoride (or of hydrofluoric acid), not of fluoride ions

29th page (page nr. 6): in the expression for KF, the exponent for Ions should be 0.5 (or 1/2) and not 1.5.

30th page (page nr. 7): "Every constant are corrected by the hydrostatic pressure" should read "All the constants are corrected for the effect of hydrostatic pressure"

Guy Munhoven
Liège, 9th October 2020

Implementation and assessment of a carbonate system model (Eco3M-CarbOx v1.1) in a highly-dynamic Mediterranean coastal site (Bay of Marseille, France).

Katixa Lajaunie-Salla[1], Frédéric Diaz[1], Cathy Wimart-Rousseau[1], Thibaut Wagener[1], Dominique Lefèvre[1], Christophe Yohia[2], Irène Xueref-Remy[3], Brian Nathan[3], Alexandre Armengaud[4], Christel Pinazo[1]

[1]Aix Marseille Univ., Université de Toulon, CNRS, IRD, MIO, UM 110, 13288, Marseille, France
[2]Aix Marseille Univ., CNRS, IRD, OSU Institut Pythéas, 13288, Marseille, France

[3]Aix Marseille Univ., Université d'Avignon, CNRS, IRD, IMBE, Marseille, France
[4]AtmoSud : Observatoire de la qualité de l'air en région Sud Provence Alpes Côte d'Azur, le Noilly Paradis, 146 ~~Rue~~rue Paradis, 13294 Marseille, Cedex 06, France

Correspondance to : Katixa Lajaunie-Salla (katixa.lajaunie-~~salla@mio.osupytheas.fr~~@gmail.com), Frédéric Diaz (frederic.diaz@univ-amu.fr)

Abstract. A carbonate chemistry balance module was implemented into a biogeochemical model of the planktonic food web. The model, named Eco3M-CarbOx includes 22 state variables that are dispatched into 5 compartments: phytoplankton, heterotrophic bacteria, detrital particulate organic matter, labile dissolved organic and inorganic matter. This model is applied to and evaluated in the Bay of Marseille (BoM, France) that is a coastal zone impacted by the urbanized and industrialized Aix-Marseille Metropolis, and subject to significant increases in anthropogenic emissions of CO_2.

The model was evaluated over the year 2017 ~~that is a period~~ for which *in situ* data of carbonate system are available in the study site. The biogeochemical state variables of the model only change with time, to represent the time evolution of a sea surface water cell in response to the implemented realistic forcing conditions. The model correctly simulates the values ranges and seasonal dynamics of most of variables of carbonate system except ~~Total Alkalinity.~~for the total alkalinity. Several numerical experiments were ~~also~~ conducted to test the response of carbonate system to (i) a seawater temperature increase, (ii) wind events, (iii) Rhône River plume ~~intrusion~~intrusions and (iv) levels of atmospheric CO_2 contents. This set of numerical experiments shows that the Eco3M-CarbOx model provides expected responses in the alteration of the marine carbonate balance regarding each of the considered perturbation. When the seawater temperature changes quickly, the behaviour of the BoM waters alters within a few days from a source of CO_2 to the atmosphere to a sink into the ocean. Moreover, the higher the wind speed is, the higher the air-sea CO_2 gas exchange fluxes are. The river intrusions with nitrate ~~and alkalinity~~ supplies lead to a decrease in the pCO_2 value, favouring the conditions of a sink for atmospheric CO_2 into the BoM. A scenario of high atmospheric concentrations of CO_2 also favours the conditions of a sink for atmospheric CO_2 into the waters of the BoM. Thus the model results suggest that external ~~forcing~~forcings have an important impact on the carbonate equilibrium in this coastal area.

1. Introduction

Current climate change mostly originates from the carbon dioxide (CO_2) increase in the atmosphere at a high annual rate (+2.63 ppm from May 2018 to May 2019, https://www.esrl.noaa.gov/gmd/ccgg/trends/global.html). This atmospheric CO_2 increase impacts the carbonate chemistry equilibrium of the oceanic water column (Allen et al., 2009; Matthews et al., 2009). Oceans are known to act as a sink for anthropogenic CO_2, *i.e.* 30% of emissions, which leads to a marine acidification (Gruber et al., 2019; Orr et al., 2005; Le Quéré et al., 2018).

CO_2 is a key molecule in the biogeochemical functioning of the marine ecosystem. Photo-autotrophic organisms, mainly phytoplankton and macro-algae, fix this gas through photosynthesis in the euphotic zone and, in turn, produce organic matter and dissolved oxygen. Heterotrophic organisms, mainly heterotrophic protists and metazoans consume organic matter and dissolved oxygen by aerobic respiration and, in turn, produce CO_2. In the Ocean, the main processes regulating CO_2 exchanges between the atmosphere and sea are the solubility pump and the biological pump at different time-scales. Overall, the thermohaline gradients drive the solubility pump, while the metabolic processes of gross primary production and respiration set the intensity of the biological pump (Raven and Falkowski, 1999).

The coastal zones, despite their small surface area and volume compared to those of the open ocean, have a large influence upon carbon dynamics and represent 14 to 30% of the oceanic primary production (Gattuso et al., 1998). At the interface between open-ocean and continents, these zones receive large inputs of nutrients and organic matter from rivers, groundwater discharge, and from atmospheric depositions (Cloern et al., 2014; Gattuso et al., 1998). On the coastline, coastal areasOn coasts, shorelines are subject to an increasing density of population and associated urbanization (Small and Nicholls, 2003). This rapid alteration of the coastlineshorelines all over the world accelerates the emissions of greenhouses gases near the coastal ocean, and it also involves large discharges of material into the seawater by wastewater runoff and/or rivers (Cloern, 2001). These anthropogenic forcing alter the biogeochemical functioning of these zones and could lead to a growing eutrophication (Cloern, 2001). Moreover, these forcing could affect the carbonate chemistry dynamics and amplify or attenuate the acidification in coastal zones. This alteration of the marine environment may provoke further changes in the structure of the plankton community, including *in fine* consequences on the populations with high trophic levels, such as teleosts (Esbaugh et al., 2012). At the global scale, coastal zones are considered to be a significant sink for atmospheric CO_2, with an estimated flux converging to 0.2 PgC y^{-1} (Roobaert et al., 2019). However, some studies highlight that the status of these areas as a net sink or source still remains uncertain due to the complexity of the interactions between biological and physical processes, and also due to the lack of *in situ* measurements (Borges and Abril, 2011; Chen et al., 2013; Chen and Borges, 2009). Moreover, the capacity for coastal zones to absorb atmospheric CO_2 resulting from the increasing human pressure also remains poorly known. There are few works which highlight, under future atmospheric CO_2 levels, that shallow seaswhether coastal zones will become a net sink or a reduced source of CO_2 (Andersson and Mackenzie, 2012; Cai, 2011).

The current increase in the atmospheric CO_2 partial pressure (pCO_2) in the surface ocean is slowly shifting the marine carbonate chemistry equilibrium towards increases in the seawater pCO_2 and bicarbonate ions (HCO_3^-) and decreases in pH and carbonate ions (CO_3^{2-}) (Hoegh-Guldberg et al., 2018). These trends were already described in several coastal and open-ocean locations worldwide (Cai et al., 2011). In a coastal Northwestern Mediterranean site, a 10-year time-series of *in situ* measurements highlights a trend of pH decrease and pCO_2 increase (Kapsenberg et al., 2017). Low pH values can inhibit the ability of many marine organisms to form the calcium carbonate ($CaCO_3$) used in the making of skeletons and shells (Gattuso et al., 2015). In an extreme case, this shift may promote dissolution of $CaCO_3$ because the water will become under-saturated with respect to $CaCO_3$ minerals (Doney et al., 2009).

The present study is dedicated to the implementation of a carbonate system module into a preexisting biogeochemical model of planktonic food web. This new model, named Eco3M-CarbOx (v1.1) is then evaluated in a highly-dynamic

2

Mis en forme : Centré

79 coastal site, *i.e.* Bay of Marseille (BoM) in the Northwestern Mediterranean Sea. This evaluation is performed on the
80 seasonal dynamics of biogeochemical and carbonate modeled variables against that of the corresponding *in situ* data
81 available over the year 2017. This study is extended by a fine analysis of the variability of the marine carbonate system
82 (stocks, fluxes) in relation to physical (*e.g.* wind events, river intrusions, temperature increases, changes in the
83 atmospheric pCO$_2$ levels) and biogeochemical processes (gross primary production (GPP) and respiration (R)) in the
84 study site. The BoM is suitable to this kind of study because this coastal area is subject to high emissions of atmospheric
85 CO$_2$ from the nearby urban area, and it also receives effluents from the Aix-Marseille metropolis. In addition, strong
86 wind events (Mistral) regularly occur, which could lead to (i) strong latent heat losses at the surface (Herrmann et al.,
87 2011) and upwelling along the coast with a common consequence of cooling effect and (ii) ~~Rhone~~Rhône River plume
88 intrusion under specific wind conditions (Fraysse et al., 2013, 2014). In this regional context, many anthropogenic
89 forcing can interact with the dynamics of the carbonate systems. Natural determinants of the composition of the marine
90 planktonic community can also play a crucial role in these dynamics.

91 **2.   Materials & Methods**

92 **2.1   Numerical model description**

93 The Eco3M-CarbOx biogeochemical model was developed to represent the dynamics of the seawater carbonate system
94 and plankton food web in the BoM. The model was implemented using the Eco3M (Ecological Mechanistic and
95 Modular Modelling) platform (Baklouti et al., 2006). The model structure used is based on an existing model of the
96 plankton ecosystem (Fraysse et al., 2013), including a description of Carbon (C), Nitrogen (N) and Phosphorus (P)
97 marine biogeochemical cycles. The Eco3M-CarbOx model includes 22 prognostic state variables that are split into 5
98 compartments: phytoplankton, heterotrophic bacteria, detrital particulate organic matter, labile and semi-labile
99 dissolved organic matter, nutrients (ammonia, nitrate and phosphate), dissolved oxygen, and carbonate system
100 variables (Fig. 1). In this study, the state variables of the Eco3M-CarbOx model only change along time (*i.e.* usually
101 termed "model 0D"), they are representative of the time evolution of a sea surface water cell but this biogeochemical
102 model is not coupled with a hydrodynamic model.
103 The model presented in this study includes a set of new developments and improvements in the realism of the plankton
104 web structure and process formulations compared to the model of Fraysse et al. (2013). In order to improve the
105 representation of chlorophyll concentration in the Bay of Marseille the phytoplankton is divided in two groups: one
106 with some ecological and physiological traits of the *Synechococcus* cyanobacteria, which is one of the major
107 constitutive members of pico-autotrophs in Mediterranean Sea (Mella-Flores et al., 2011), and another with traits of
108 large diatoms, which are generally observed during spring blooms at mid-latitudes (Margalef, 1978). For both of the
109 phytoplankton, there is a diagnostic chlorophyll-a variable related to the phytoplankton C-biomass, the phytoplankton
110 N-to-C ratio, and the limiting internal ratio f_Q^N (Faure et al., 2010; Smith and Tett, 2000; Tab. B2, Appendix B). The
111 functional response of primary production was modified using another formulation of temperature limitation function
112 which takes into account the optimal temperature of growth for each phytoplankton group. The exudation of
113 phytoplankton was modified taking into account the intracellular phytoplankton ratio. For the uptake of matter by
114 bacteria and the remineralization processes the dependence on intracellular bacteria ratio was modified. A temperature
115 dependence of all biogeochemical processes was added to take into account the effects of rapid and strong variations
116 of seawater temperature on plankton during episodes of upwelling for instance that are usually observed in the BoM.
117 Also certain parameters in some formulations were modified owing to the alterations of some formulations. (Tabs. B4
118 & B5, Appendix B).

Mis en forme : Centré

119 Additionally, a carbonate system module was developed and three state variables were added: dissolved inorganic
120 carbon (DIC), total alkalinity (TA) and the calcium carbonate ($CaCO_3$) implicitly representing calcifying organisms.
121 The knowledge of DIC and TA allows the calculation of the pCO$_2$ and pH (total pH scale) diagnostic variables,
122 necessary for resolving all the equations of the carbonate system. These equations use apparent equilibrium constants,
123 which depend on temperature, pressure, and salinity (Dickson, 1990a, 1990b; Dickson and Riley, 1979; Lueker et al.,
124 2000; Millero, 1995; Morris and Riley, 1966; Mucci, 1983; Riley, 1965; Riley and Tongudai, 1967; Uppström, 1974;
125 Weiss, 1974). The details of the resolution of carbonate system module are given in the Appendix A. For this module
126 three processes were also added: the precipitation and dissolution of calcium carbonate and the gas exchange of pCO$_2$
127 with the atmosphere. Based on the review of Middelburg (2019), it is considered that: (i) TA decreases by 2 moles for
128 each mole of $CaCO_3$ precipitated, by 1 mole for each mole of ammonium nitrified, by 1 mole for each mole of
129 ammonium assimilated by phytoplankton, and TA increases by 2 moles for each mole of $CaCO_3$ dissolved, and by 1
130 mole for each mole of organic matter mineralized by bacteria in ammonium (SeeTab. B2, Appendix B Tab. B2). (ii)
131 DIC is consumed during the photosynthesis and calcification processes and is produced by respiration (of
132 phytoplankton, zooplankton, and bacteria) and the $CaCO_3$ dissolution processes. Moreover, the dynamics of DIC are
133 altered by the CO$_2$ exchanges with the atmosphere (Tab. B2, Appendix B). The air-sea CO$_2$ fluxes are calculated from
134 the pCO$_2$ gradient across the air-sea interface and the gas transfer velocity (Tab. B3, Appendix B) estimated from the
135 wind speed and using the parametrization of Wanninkhof (1992).
136 In the Eco3M-CarbOx model, zooplankton is considered as an implicit variable. However, a closure term based on the
137 assumption that all of the matter grazed by the zooplankton and higher trophic levels returns as either organic or
138 inorganic matter by excretion, egestion and mortality processes is taken into account (Fraysse et al., 2013). The model
139 considers a "non-redfieldian" stoichiometry for phytoplankton and bacteria. All the biogeochemical model
140 formulations, equations and associated parameters values are detailed in the Appendix B.

141 **2.2   Study area**

142 The BoM is located in the eastern part of the Gulf of Lions, in the Northwestern Mediterranean Sea (Fig. 2). The city
143 of Marseille, located on the coast of the BoM, is the second largest city of France, with a population of *ca*. 1 million.
144 The RhoneRhône River, which flows into the Gulf of Lions, is the greatest source of freshwater and nutrients for the
145 Mediterranean Sea, with a river mean flow of 1800 m^3 s^{-1} (Pont et al., 2002). Several studies highlight the eastward
146 intrusion events from the RhoneRhône River plume in the BoM under East and South-easterly wind conditions, which
147 favor biological productivity (Fraysse et al., 2014; Gatti et al., 2006; Para et al., 2010). The biogeochemistry of the
148 BoM is complex and highly driven by hydrodynamics. For example, North-Northwesterly winds induce upwelling
149 events which bring upward cold and nutrient-rich waters (Fraysse et al., 2013). Moreover, the oligotrophic Northern
150 Current occasionally intrudes into the BoM (Petrenko, 2003; Ross et al., 2016).
151 Despite the presence of several marine protected areas around the BoM (the Regional Park of Camargue, the Marine
152 protected area Côte Bleue and the National Park of Calanques), it is strongly impacted by diverse anthropogenic
153 forcing, because industrialized and urbanized areas are located all along the coast. From the land, the BoM receives
154 nutrients and organic matter from the urban area of the Aix-Marseille metropolis (Millet et al., 2018), the industrialized
155 area of Fos-sur-Mer (one of the biggest oil-based industry areas in Europe), and the Berre Lagoon, which is eutrophized
156 (Gouze et al., 2008; Fig. 2C). From the atmosphere, the BoM is subject to fine particles deposition and greenhouse gas
157 emissions (including CO$_2$) from the nearby urban area, and it also receives effluents from the Aix-Marseille metropolis.

158 **2.3   Dataset**

Mis en forme : Centré

159 The modelled variables of the carbonate system (DIC, TA, pH and pCO$_2$) and chlorophyll-a are hereafter compared to

160 observations collected at the SOLEMIO station (Figs. 2C & 3), which is a component of the French national monitoring

161 network (Service d'Observation en Milieu Littoral - SOMLIT, http://somlit.epoc.u-bordeaux1.fr/fr/). Major

162 biogeochemical parameters have been recorded since 1994. Carbonate chemistry variables (pH, pCO$_2$, DIC and TA)

163 have been available since 2016, every two weeks.

164 **2.4   Design of numerical experiments**

165 In the present work, the Eco3M-CarbOx model was run for the whole year of 2017. This year was chosen because *in*

166 *situ* data of carbonate systems (DIC, TA, pH and pCO$_2$) are available for the whole year at the SOLEMIO station (Fig.

167 2C). The biogeochemical variables were initialized using *in situ* data from winter conditions (Tab. B1, Appendix B).

168 The model was forced by time-series of sea surface temperature and salinity, wind (at 10 m), light, and atmospheric

169 CO$_2$ concentrations. The sea temperature time-series is from *in situ* hourly data recorded at the Planier station (Fig.

170 2C). For salinity, hourly *in situ* data from the SOLEMIO station and from the CARRY buoy were used (Fig. 2C). Wind

171 and light hourly time-series were extracted from the WRF meteorological model at the SOLEMIO station (Yohia,

172 2017). Finally, we used hourly atmospheric CO$_2$ values from *in situ* measurements recorded at the *Cinq Avenues* station

173 (CAV station, Fig. 2B) by the AtmoSud Regional Atmospheric Survey Network, France (https://www.atmosud.org).

174 This simulation is the reference simulation (noted S0). As highlighted previously, ~~Rhone~~Rhône River plume intrusions

175 (due to wind-specific conditions) have an impact on the dynamics of primary production (Fraysse et al., 2014; Ross et

176 al., 2016) and then on the seawater ~~CO$_2$ concentrations.~~carbonate system. Moreover, the seawater temperature and

177 atmospheric CO$_2$ variations control the seawater CO$_2$ dynamics *via* the solubility equilibrium and gas exchange with

178 the atmosphere (Middelburg, 2019). In order to quantify the impact of different forcing, several simulations (hereafter

179 noted S), which are summarized in Table 1, were conducted:

180 ● Impact of seawater temperature increase, S1: the forcing time-series of *in situ* temperatures was shifted by +1.5°C

181   (Cocco et al., 2013).

182 ● Impact of wind events: a first simulation S2 was run with a constant wind intensity of 7 m s^{-1} (2017 annual average

183   wind speed) throughout the year and a second one (S3) with two three-day periods of strong wind speed (20 m s^{-1})

184   representative of short bursts of Mistral (data not shown) starting on May 15th and August 15th, and a constant value

185   of 7 m s^{-1} the rest of the year.

186 ~~●~~ Impact of ~~Rhone~~nutrient supply (nitrate) during a Rhône River plume intrusion (~~a salinity~~S4). A threshold of 37

187   has been chosen to identify the presence of low-salinity waters from the ~~Rhone~~Rhône River plume~~):~~

188 ~~●~~ Nitrate inputs were simulated ~~during~~ in ~~the~~ ~~river plume intrusions (S4):~~forcing file of salinity. Here, the

189   ~~level~~contents of nitrate supplied by the river depends on the salinity ~~level~~. A relationship between these two

190   variables was then established ~~using NO$_2$ and salinity data at~~for the SOLEMIO point from the MARS3D-RHOMA

191   coupled physical and biogeochemical model (Fraysse et al., 2013; Pairaud et al., 2011)~~, which~~. This relationship

192   has already been used successfully to reproduce realistic observed conditions in the studies of Fraysse et al. (2014)

193   and Ross et al. (2016): NO$_{3intrusion}$ (mmol m^{-3}) = -1.~~7~~70×S + 65.

194 ~~TA inputs were simulated during river plume intrusions (S5): the level of TA supply by the river depends on~~

195   ~~the salinity. A relationship was established using *in situ* data from the SOLEMIO station during river intrusion:~~

196   ~~TA$_{intrusion}$ (μmol kg^{-1}) = -21.0×S + 3400.~~

197 ● Non-urban atmospheric CO$_2$ concentrations (~~S6~~S5): this simulation takes into account the forcing of atmospheric

198   CO$_2$ values measured at the *Observatoire de Haute Provence* station (OHP, Fig. 2B) located outside of the Aix-

Mis en forme : Couleur de police : Couleur personnalisée(RVB(35;31;32))

Mis en forme : Retrait : Gauche : 0 cm, Suspendu : 0,5 cm, Hiérarchisation + Niveau : 1 + Style de numérotation : Puce + Alignement : 1,26 cm + Retrait : 1,9 cm

Mis en forme : Centré

199   Marseille metropolis from the ICOS National Network, France (http://www.obs-hp.fr/ICOS/Plaquette-ICOS-
200   201407_lite.pdf).

201 In this work, we calculated the daily mean values of state variables, ~~the~~ statistical parameters and mean fluxes of
202 modeled processes throughout the year and over two main hydrological periods: the stratified and mixed water column
203 periods. The stratified water column (SWC) is defined with a temperature difference between the surface and bottom
204 of more than 0.5°C (Monterey and Levitus, 1997). For the simulated year (2017), the SWC period lasts from May 10th
205 to October 20th. The mixed water column (MWC) period corresponds to the rest of the year.

3. Results

3.1 Model skills

208 Following the recommendations of Rykiel (1996), three criteria were considered to evaluate the performance of our
209 model:
210   -   Does the model reproduce the timing of the observed variations of carbonate system at the seasonal time
211   scale?
212   -   Does the model reproduce the observed pCO_2 and pH ranges at the seasonal time scale?
213   -   Analysis of the Willmott Skill Score (WSS): this index is an objective measurement of the degree of
214   agreement between the modeled results and the observed data. A correct representation of observations by
215   the model is achieved when this index is higher than 0.70 (Willmott, 1982).
216 Over most of the studied period, the model simulates lower chlorophyll-a concentrations than the *in situ* observations,
217 especially during the MWC period (Fig. 3A). Two maxima of chlorophyll-a concentrations are observed *in situ:* the
218 first one at *ca.* 1.71 mg m^{-3} in March and the second one at *ca.* 0.68 mg m^{-3} in May. They are both linked to ~~Rhone~~Rhône
219 River plume intrusions. Several *in situ* maxima between 0.50 and 0.70 mg m^{-3} are observed between March and April
220 (at the end of the MWC period), and they signaled the spring bloom event (Tab. 2 & Fig. 3A). The biogeochemical
221 model quantitatively reproduces the spring bloom observed at the end of the MWC period (Fig. 3A) with a maximum
222 value of *ca.* 0.69 mg m^{-3}. The model does not catch the two aforementioned maxima of chlorophyll, and it contains a
223 low WSS and a strong bias (0.37 and +0.22 mg m^{-3}, respectively - Tab. 2).
224 On the whole, the seasonal variations of the seawater pCO_2 are correctly simulated by the biogeochemical model (Fig.
225 3B), even if the values are rather overestimated during the MWC period. From January to February, the model
226 reproduces the slight decrease in the observed pCO_2 and from February to March the increase in pCO_2 even if the latter
227 modelled remains smaller. In mid-April, during the simulated spring bloom period, the observed drop in pCO_2 and
228 increase in pH are also spotted in the model (Fig. 3B & 3C). The model especially succeeds in reproducing the observed
229 increase in relation to high temperatures during the SWC period. The reduction of the CO_2 solubility due to thermal
230 effects mostly explains the increase in pCO_2 during the SWC period. The strong standard deviation of modeled values
231 during the SWC period can be explained by the rapid changes in temperature probably due to upwelling usually
232 occurring at this time of the year (Millot, 1990). The range of modeled pCO_2 values (345 - 503 µatm) encompasses
233 the range of observed values (358 - 471 µatm; Tab. 2). The statistical analysis provides a mean bias of +23 µatm, and
234 a WSS of 0.69 (Tab. 2).
235 The seasonal dynamic of pH is mostly reproduced by the model, and in particular, the decrease during the SWC period
236 (Fig. 3C). However, the modelled pH is generally underestimated throughout the year, except during the SWC period,
237 with a mean bias of -0.015 (Tab. 2). The seasonal range is captured by the model with a minimum value during the

Mis en forme : Centré

238 SWC period (7.994 *vs.* 8.014 for observations; Tab.2) and a maximum one during the MWC period (8.137 *vs.* 8.114
239 for observations; Tab.2). The statistical analysis highlights an index of agreement between the *in situ* data and the
240 model outputs higher than 0.70 (Tab. 2).

241 The seasonal variations of DIC show the highest values during the MWC period and a decrease (resp. increase) during
242 the beginning (resp. the end) of the SWC period (Fig. 3D). The lowest values are observed during September. The
243 Eco3M-CarbOx model closely matches the seasonal dynamic by reproducing the range of extreme observed values
244 (Tab. 2). The mean bias is also small (-8.48 μmol kg^{-1}, Tab. 2). More than 70% (0.73, Tab. 2) of modeled DIC
245 concentrations are in statistical agreement with the corresponding observations.

246 The seasonal cycle of measured TA does not show a clear pattern (Fig. 3E). Large variations of values ranging between
247 2561 and 2624 μmol kg^{-1} (Tab. 2) are observed, whatever the hydrological season is that is considered. The
248 biogeochemical model provides almost constant values around 2570 μmol kg^{-1} all along the year, which is lower than
249 *in situ* data. With a low WSS index of agreement and a large mean bias (Tab. 2), the model is not able to confidently
250 reproduce the observed variations of TA (Fig. 3E & Tab. 2).

251 ### 3.2   Carbon fluxes and budgets

252 For the year 2017, the values of temperature vary between 13.3°C and 25.9°C (Fig. 4A). The DIC variations closely
253 match those of temperature (correlation coef. -0.75). For example, the spring increase in temperature leads to a decrease
254 in DIC concentrations (Figs. 4A & 4C), and the minimum values are reached at the end of SWC period. Over the
255 simulated period, the air-sea CO_2 fluxes (F_{aera}) vary between -14 and 17 mmol m^{-3} d^{-1}, with a weakly positive annual
256 budget of +6 mmol m^{-3} y^{-1} (or +0.017 mmol m^{-3} d^{-1}, Tab. 3). Then, the BoM waters would act as a net source of CO_2
257 to the atmosphere on an annual basis. However, on a seasonal basis, the BoM waters would change from a net sink
258 during the MWC period (F_{aera} <0; Tab. 3) to a net source during the SWC one (F_{aera} >0; Tab. 3).

259 On an annual basis, the gross primary production (GPP) and total respiration (R) are balanced, leading to a null average
260 net ecosystem production (NEP, NEP=GPP-R) (Fig. 4F & Tab. 3). The intensity of autotroph respiration (R_a) is lower
261 than that of primary production (annual mean of 0.065 *vs.* -0.413 mmol m^{-3} d^{-1}, respectively - Tab. 3). While the
262 zooplankton and bacterial respiration account for an average of 0.348 mmol m^{-3} d^{-1} (Tab. 3). On a seasonal basis, the
263 model highlights an ecosystem dominated by autotrophy during the MWC period (NEP>0; Tab. 3) and heterotrophy
264 during the SWC period with higher fluxes values (NEP<0; Tab. 3). The biogeochemical fluxes show the strongest
265 variations along the SWC period, following those of temperature (Fig. 4F). The maximum GPP occurs in April and is
266 correlated with the maximum chlorophyll concentration. At this time, the ecosystem is autotroph (NEP>0; Figs. 4B &
267 4F), and is a net sink for atmospheric CO_2, which explains the DIC and seawater pCO$_2$ decreases during the bloom
268 period (Figs. 4C, 4D & 4E)

269 When looking in details at the temperature and salinity 2017 time-series (Fig. 4A), several crucial events can be seen
270 occurring, including freshwater intrusions (*e.g.* ~~15~~ March 15th and ~~6~~ May 6th) into the BoM and large variations of
271 temperature in relation with upwelling events or latent heat losses due to wind bursts. The largest freshwater intrusion
272 from the ~~Rhone~~ Rhône River plume occurs in mid-March, with a minimum observed salinity of *ca.* 32.5 at the
273 SOLEMIO station (Fig. 4A). During this event, the seawater pCO$_2$ decreases and pH increases concomitantly (Figs.
274 4C & 4D). Then, seawater appears to be temporarily under-saturated in CO_2 and the BoM waters thus acts as a sink
275 for atmospheric CO_2 at the time of intrusion (Fig. 4E).

276 During the SWC period, upwelling events quickly cool the surface seawater. In two days, from July 25th to 27th, the
277 water temperature drops from 24.7°C to 16.9°C (Fig. 4G). The decrease in temperature corresponds to the increase in
278 DIC concentrations (Fig. 4I). Concomitantly, the values of seawater pCO$_2$ decrease from 497 to 352 μatm and pH

Mis en forme : Centré

279   increase from 7.99 to 8.12 (Figs. 4I & 4J). This event quickly changes the BoM waters from a source to a sink for

280   atmospheric CO_2 (from +17 to -14 mmol m^{-3} d^{-1}, Fig. 4K), and also from a net heterotroph to a net autotroph ecosystem

281   (Fig. 4L).

282   **3.3   Impact of external forcing on the dynamics of carbonate system**

283   **3.3.1   Temperature increase**

284   Here we compare the reference simulation S0 with the S1 simulation (seawater temperature elevation of 1.5°C - Fig.

285   5). During the year, there are few changes on the carbonate system variables such as the pCO_2 and pH (data not shown).

286   The main alterations occur during the blooms of phytoplankton. The simulated bloom of phytoplankton occurs later,

287   at beginning of May, for both diatoms and picophytoplankton, with a maximum value of chlorophyll at1.4 and 0.4 mg

288   m^{-3}, respectively (Figs. 5A & 5F).

289   As both the limitations due to light and nutrients remain about the same during the simulations S0 and S1, this

290   counterintuitive occurrence of bloom relative to changes in temperature is mainly explained by the temperature limiting

291   function, which depends on the optimal temperature of growth (T_{opt}). For the picophytoplankton, from January to April,

292   the increase of 1.5°C drastically reduces the limitation by temperature (Fig. 5C), because the temperature is closer to

293   the optimal temperature (T_{opt}=16°C, Tab. A4) during S1 than S0. In the S0 simulation, the temperature reaches T_{opt} *ca.*

294   April 15th and it induces the bloom, while at the same time in S1 the temperature moves slightly away from T_{opt} and it

295   does not enable the triggering of a bloom. At the time of the bloom in S1, the opposite configuration occurs. In S0, the

296   ambient temperature is again far from T_{opt}, explaining the absence of bloom, while in the S1 the ambient temperature

297   is closer to T_{opt} enabling the occurrence of bloom. The picophytoplankton bloom then occurs later in the warm

298   simulation S1 than in the reference simulation S0 (Fig. 5A). The duration and termination of bloom is controlled both

299   by the nutrients availability and the temperature (Figs. 5C & 5D). Inversely, from January to April, the diatoms' growth

300   limitation by temperature is strengthened in the warm simulation S1 (Fig. 5H), because the resulting ambient

301   temperature is further from the optimum temperature (T_{opt}=13°C, Tab. A4) than that in the reference simulation S0.

302   This induces a slower growth of diatoms and a delay of the maximum concentration (Fig. 5F). Afterwards the

303   photosynthesis is mainly limited by temperature (Fig. 5H).

304   The ecosystem is net autotroph at the time of blooms whatever the simulation considered (NEP>0; Fig. 5E) and the

305   quantity of DIC (not shown) fixed through autotroph processes is larger than that released by heterotroph processes.

306   During the short period of bloom, the seawater pCO_2 decreases, leading to some negative air-sea fluxes (*i.e.* an oceanic

307   sink for atmospheric CO_2). In the warm simulation, the later occurrence of bloom enables the period of the spring sink

308   to extend by *ca.* three weeks over May relative to the reference simulation (Fig. 5J).

309   **3.3.2   Wind speed**

310   The Bay of Marseille is periodically under the influence of strong wind events (Millot, 1990). Here we compare two

311   simulations: one with a constant wind value (S2) and the other one with two wind events that occur in May and August

312   (S3) (Figs. 6A & D). The result of this numerical experiment shows that the stronger the wind speed is, the higher the

313   air-sea fluxes are, mainly owing to the increase in gas transfer velocity. Depending on the gradient of CO_2 between

314   seawater and the atmosphere, strong wind speeds will favor either the emission or uptake of CO_2 (Figs. 6B & E). In

315   May, with the air-sea CO_2 flux being positive, the outgassing of CO_2 to the atmosphere is enhanced leading to a

316   decrease in seawater pCO_2 (Fig. 6C). On the contrary, in August the oceanic sink of atmospheric CO_2 is amplified

317   which leads to an increase in the seawater pCO_2 value (Fig. 6F).

Mis en forme : Centré

3.3.3 Supply in nitrate ~~and alkalinity~~ by river inputs

According to the model results (Fig. 7), the occasional inputs of nitrate (S4) that are linked to ~~Rhone~~Rhône River plume intrusions favor primary production and they led to increased chlorophyll concentrations (Figs. 7B & 7C) five times during the SWC period. These blooms, as seen previously, lead to a decrease (resp. increase) in the seawater pCO$_2$ (resp. pH) (Figs. 7E & 7F). It can be noted that with the strongest river supply at mid-March (Figs. 7A & 7B) the occurrence of the spring bloom is earlier (Fig. 7C) than that occurring in the reference simulation (S0). The time lag between river nutrient supply and bloom is due to the temperature limitation (Fig. 4C). During blooms occurring within the SWC period following intrusions, the DIC concentrations are generally lower than those of the reference simulation, as in the case of the bloom of mid-May (decrease by ca. 15 µmol kg^{-1}, Fig. 7J), due to the autotroph processes dominating the heterotroph ones. In turn, the seawater pCO$_2$ drops by ca. 30 µatm (Fig. 7K) and pH increases by ca. 0.030 (Fig. 7L). Nitrate inputs, favoring primary production, reduce the source of CO$_2$ to the atmosphere ~~or~~and intensify the sink of atmospheric CO$_2$ into the waters of BoM (~~Fig~~Figs. 7E & 7K).

~~The supply of alkalinity during the Rhone River plume intrusions (Fig. 8A) significantly increases the DIC concentrations (ca. +50 µmol kg^{-1}, Figs. 8B & 8F), in every hydrological period considered. During the strongest freshwater input at mid-March, the sharp TA increase by ca. +150 µmol kg^{-1} (Fig. 8E) leads to a large pCO$_2$ drop by ca. 92 µatm and a pH increase by 0.13 (Figs. 8G & 8H). The air-sea gradient of pCO$_2$ increases at mid-March, favoring sink conditions for atmospheric CO$_2$ into the waters of the BoM (Fig. 8G).~~

3.3.4 Urban air CO$_2$ concentrations

The Aix-Marseille metropolis is strongly subject to urban emissions to the atmosphere (Xueref-Remy et al., 2018a). The seasonal variability of atmospheric CO$_2$ concentrations at the urban site (CAV station, Fig. 2) is much higher than that observed in a non-urban area (OHP station, Fig. 2), especially during the MWC period (Fig. ~~9A~~8A): CO$_2$ concentrations vary between 379 and 547 µatm at the CAV station and between 381 and 429 µatm at the OHP station. Moreover, in winter the atmospheric pCO$_2$ is higher in the urban area than non-urban area, whereas in summer those of both areas are quite close. These differences in the seasonal pattern and between areas are usually explained by (i) the thinner atmospheric boundary layer, (ii) the decreased fixation of CO$_2$ by terrestrial vegetation, and (iii) the greater influence of anthropogenic activities by emissions from heating (Xueref-Remy et al., 2018b). Forcing the model by atmospheric pCO$_2$ values from urban or non-urban site can lead to significant differences in the values of the seawater pCO$_2$ during the MWC period especially. The air-sea gradient of pCO$_2$ is higher when using a forcing derived from the CO$_2$ concentrations originating from an urban area than from non-urban area, which strengthens the sink of atmospheric CO$_2$ into the waters of BoM. The seawater pCO$_2$ is then lower with non-urban area pressure (~~S6~~S5) than with urban area pressure (S0), because of lower CO$_2$ solubility in the BoM (Fig. ~~9B~~8B).

4. Discussion

4.1 Model performance

The evaluation of model skill vs. in $situ$ data highlights that the modeled pH, pCO$_2$, DIC are in acceptable agreement with observations (Fig. 3). The seasonal variations observed for the different variables are captured by the model, including for example the seasonal decrease in DIC and pH during the SWC period, in relation to the increase in pCO$_2$, and the inverse scenario during the MWC period. The chlorophyll content variability is not well reproduced, especially during spring (Fig. 3A), even taking into account the nitrate supply from the ~~Rhone~~Rhône River plume intrusion (Fig. 7C). This is due to the multiple origins of chlorophyll, organic matter, and nutrients in the BoM that are not accounted

357 for in the Eco3M-CarbOx model: autochthonous marine production, and allochthonous origins from the ~~Rhone~~Rhône

358 and Huveaune River plumes (Fraysse et al., 2013). The observed variations and levels of TA are not correctly simulated

359 by the model (Fig. ~~3F), even taking into account the supply of TA coming from the Rhone River plume (Fig. 8). The~~

360 ~~formulation used in this study for TA inputs from rivers needs to be refined and compared with other works (Gemayel~~

361 ~~et al., 2015; Schneider et al., 2007).~~3F). The study of Soetaert et al. (2007) highlights that the main variations of TA

362 in the marine coastal zones are linked to freshwater supplies and marine sediments. The present study does not take

363 into account the inputs of TA from the Rhône River and the water-sediment interface, and it may explain why the TA

364 variable is not correctly predicted by our model.

4.2 Contribution of physical and biogeochemical processes to the variability of carbonate system

366 The contribution of each biogeochemical process to the DIC variability can be assessed using the presented model: the

367 aeration process contributes to 78% of the DIC variations and biogeochemical processes together to 22% (Tab. 3). As

368 mentioned by Wimart-Rousseau et al. (2020), the model suggests that the seawater pCO_2 variations and associated

369 fluxes would be mostly driven by the seawater temperature dynamics. Moreover, the seasonal variations of the air-sea

370 CO_2 flux are in agreement with some previous field studies (De Carlo et al., 2013; Wimart-Rousseau et al., 2020),

371 which measured a weak oceanic sink for atmospheric CO_2 during winter and a weak source to the atmosphere during

372 summer.

373 The model results reveal that temperature would play a crucial role in controlling two counterbalanced processes: (1)

374 the carbonate system equilibrium and (2) the phytoplankton growth. The increase in temperature during SWC leads to

375 a higher pCO_2 in seawater due to the decrease in the CO_2 solubility (Middelburg, 2019) and, at the same time, the

376 fixation of DIC by phytoplankton is favored, leading to a decrease in the pCO_2 level. The imbalance between the latter

377 two processes leads to a change in the ecosystem status (autotrophic or heterotrophic) and the corresponding behavior

378 as a sink or source to the atmosphere. In case of a 1.5°C rise over the whole year, the temperature variation has a very

379 small impact on the carbonate system dynamics. However, it favors the autotrophic processes and strengthens the

380 oceanic sink of atmospheric CO_2 during the bloom of phytoplankton (Figs. 5E & 5J).

4.3 Contribution of the external forcing to the variability of carbonate system

382 In line with several previous works on the Northwestern Mediterranean Sea (De Carlo et al., 2013; Copin-Montégut et

383 al., 2004; Wimart-Rousseau et al., 2020), the model also suggests that the status of the Bay of Marseille regarding sink

384 or source for CO_2 could change at high temporal frequency (*i.e.* hours to days). Bursts of North, Northwestern winds,

385 lead to sudden and sharp decreases in seawater temperature (<2 days, Fig. 4G) either directly by latent heat loss through

386 evaporation at the surface (Herrmann et al., 2011) or indirectly by creating upwelling (Millot, 1990), with the

387 consequences of decrease in the seawater pCO_2 values (Fig. 4J) and *in fine*, an alteration of the CO_2 air-sea fluxes.

388 Model results suggest that the fast variations of temperature could lead to rapid changes of the sink *vs.* source status in

389 this coastal zone (Fig. 4K). ~~Moreover, previous study on the BoM highlights that upwelling favors ephemeral blooms~~

390 ~~of phytoplankton by nutrient supplies up to euphotic layer (Fraysse et al., 2013) and would, in turn, contribute to the~~

391 ~~seawater pCO_2 decrease.~~Moreover, Fraysse et al. (2013) highlight that upwelling in the BoM favors ephemeral blooms

392 of phytoplankton by nutrient supplies up to euphotic layer and would, in turn, contribute to the seawater pCO_2 decrease.

393 North, and Northwestern winds through latent heat losses and/or upwelling events could then enhance the sink for

394 atmospheric CO_2 due to the temperature drop and nutrients inputs. However, these results remain to be preliminary

395 because in our experimental design only the cooling effect of upwelling on the carbonate balance is taken into account.

396 But concomitantly, upwelling usually bring nutrients and DIC at the surface and these supplies could also perturb the

397 balance of the carbonate system. A next coupling of the Eco3M-CarbOx model with a tridimensional hydrodynamic
398 model would enable to certainly embrace the multiple effects of upwelling on the dynamics of the carbonate system in
399 this area and refine the results presented in this study.

400 High wind speeds (>7 m s^{-1}) amplified considerably the gaseous exchange of CO_2 (De Carlo et al., 2013; Copin-
401 Montégut et al., 2004; Wimart-Rousseau et al., 2020). The model highlights that a strong wind event of 3 days has a
402 significant impact on the seawater pCO_2 values during a longer period of ca. 15 days (Fig. 6). A combination of high
403 atmospheric pCO_2 value and high wind speed would then favor the sink for CO_2 into the waters of the BoM. The
404 aeration process depends also on the choice of the formulation of the gas transfer velocity (k_{600}). In this study, the
405 formulation of Wanninkhof (1992) is used and depends of the wind speed at 10 m above the water surface. However,
406 the current velocity could favor the gas exchange and suspended matter concentration could limit the gas exchange
407 (Abril et al., 2009; Upstill-Goddard, 2006; Zappa et al., 2003). Due to the important heterogeneity of physical and
408 biogeochemical forcings in coastal zones, other factors that control the air-sea gas exchange should certainly be taken
409 into account.

410 The simulation with intrusions of the ~~Rhone~~Rhône River plume shows that inputs of nitrate ~~and TA~~ cause a drop of
411 seawater pCO_2 ~~due~~owing to ~~some two concomitant effects:~~ nutrients supply ~~favors~~favoring the phytoplankton
412 development ~~and TA inputs~~(Fig. 7). In this scenario, the oceanic sink of atmospheric CO_2 is enhanced. But rivers also
413 supply TA (e.g. Gemayel et al., 2015; Schneider et al., 2007) and DIC (e.g. Sempéré et al., 2000) that shift the carbonate
414 system equilibrium ~~leading to~~toward a pCO_2 decrease and a DIC increase (Middelburg, 2019) ~~(Figs. 7 & 8). The~~
415 ~~consequence is that the oceanic sink of CO_2 is enhanced. In fact, the experimental design on the Rhone River supply~~
416 ~~only considers the TA perturbation on the carbonate system but not that due to the DIC supply. To take into account~~
417 ~~the latter supply may further impact the DIC concentration when intrusions occur and it could sensibly modify the.~~
418 Taking into account these further supplies may sensibly modify the modeled carbonate balance in the BoM. A next
419 step to the present work will be to design more realistic numerical experiments to refine the results obtained in this
420 preliminary study. The intrusions of ~~Rhone~~Rhône River plume also induce a salinity decrease of the BoM waters,
421 which leads to drop the pCO_2 levels in the model. This drop of pCO_2 is due to the decrease in the CO_2 solubility when
422 salinity decreases (Middelburg, 2019).

423 In the scenario of forcing the model by using urban atmospheric pCO_2 time-series, the air-sea gradient increases and
424 then, it enhances the status of the BoM as a sink for atmospheric CO_2. As suggested by the in situ study of Wimart-
425 Rousseau et al. (2020), the Eco3M-Carbox model highlights the crucial role of the coastal ocean in urbanized area,
426 with an increase in atmospheric CO_2, the CO_2 uptake by the costal ocean may increase. This results is in line with
427 studies of Andersson and Mackenzie (2004) and Cai (2011) that predict an increase in the intensity of CO_2 sink ~~in~~
428 ~~coastal areas due to high atmospheric CO_2 levels~~ and a potential threat to coastal marine biodiversity~~.~~ in coastal areas
429 owing to high atmospheric CO_2 levels.

430 **5. Conclusion**

431 A marine carbonate chemistry module was implemented in the Eco3M-CarbOx biogeochemical model and evaluated
432 against in situ data available in the Bay of Marseille (Northwestern Med. Sea) over the year 2017. The model correctly
433 simulates the values ranges and seasonal dynamics of most of variables of the carbonate system except ~~Total~~
434 ~~Alkalinity~~for the total alkalinity. Several numerical experiments were also conducted to test the sensitivity of carbon
435 balance to physical processes (temperature and salinity), biogeochemical processes (GPP and respiration processes)
436 and external forcing (wind, river intrusion and atmospheric CO_2). This set of numerical experiments shows that the

Mis en forme : Centré

437 Eco3M-CarbOx model provides expected responses in the alteration of the marine carbonate balance regarding each
438 of the considered perturbation.
439 On the whole, the model results suggest that the carbonate system is mainly driven by the seawater temperature
440 dynamics. At a seasonal scale, the BoM marine waters appear to be a net sink of atmospheric CO_2 and a dominant
441 autotroph ecosystem during the MWC period, and a net source of CO_2 to the atmosphere during the SWC period,
442 which is mainly characterized by a dominance of heterotroph processes. However, the model results highlight that
443 sharp seawater cooling observed within the SWC period and probably owing to upwelling events, ~~causes~~cause the CO_2
444 status of the BoM marine waters to change from a source to the atmosphere to a sink into the ocean within a few days.
445 External forcing as the temperature increases leads to a delay in the bloom of phytoplankton. Strong wind events
446 enhance the gas exchange of CO_2 with the atmosphere. A ~~Rhone~~Rhône River plume intrusion with input of nitrate ~~and~~
447 ~~alkalinity~~ favors pCO_2 decreases, and the sink of atmospheric CO_2 into the BoM waters is enhanced. The higher
448 ~~air~~atmospheric pCO_2 values from the urban area intensify the oceanic sink of atmospheric CO_2.
449 The BoM biogeochemical functioning is mainly forced by wind-driven hydrodynamics (upwelling, downwelling),
450 urban rivers, wastewater treatment plants, and atmospheric deposition (Fraysse et al., 2013). In addition, Northern
451 Current and ~~Rhone~~Rhône River plume intrusions frequently occurred (Fraysse et al., 2014; Ross et al., 2016).
452 Moreover, the BoM harbors the second bigger metropolis of France (Marseille) that is impacted by many harbor
453 activities. The next step of this study will be to couple the Eco3M-CarbOx biogeochemical model to a 3D
454 hydrodynamic model that will mirror the complexity of the BoM functioning. In this way, the contributions of
455 hydrodynamic, atmospheric, anthropic, and biogeochemical processes to the DIC variability will be able to be
456 determined with higher refinement and realism, and an overview of the air-sea CO_2 exchange could be made at the
457 scale of the Bay of Marseille. The main results of our study could be transposed to other coastal sites that are also
458 impacted by urban and anthropic pressures. Moreover, in this paper we highlighted that fast and strong variations of
459 pCO_2 values occur, so thus it is essential to acquire more *in situ* values at high frequency (at least with an hourly
460 resolution) to understand the rapid variations of the marine carbon system at these short spatial and temporal scales.
461

Mis en forme : Centré

Code availability

Eco3M is freely available under CeCILL license agreement (a French equivalent to the L-GPL license; http://cecill.info/licences/Licence_CeCILL_V1.1-US.html; last access: 10 February 2020). The Eco3M-CarbOx model is written in Fortran-90/95 and the plotting code is written in Matlab®. The exact version of the model used to produce the results presented in this paper is archived on Zenodo (DOI: 10.5281/zenodo.3757677) (last access: 24 August 2020). A short User Manual is given in the Appendix C of this study.

Mis en forme : Centré

References

Abril, G., Commarieu, M. V., Sottolichio, A., Bretel, P. and Guérin, F.: Turbidity limits gas exchange in a large macrotidal estuary, Estuar. Coast. Shelf Sci., 83, 342–348, doi:10.1016/j.ecss.2009.03.006, 2009.

Allen, M. R., Frame, D. J., Huntingford, C., Jones, C., Lowe, J. A., Meinshausen, M. and Meinshausen, N.: Warming caused by cumulative carbon emissions towards the trillionth tonne, Nature, 458, 1163–1166, doi:10.1038/nature08019, 2009.

Andersson, A. J. and Mackenzie, F. T.: Shallow-water oceans: a source or sink of atmospheric CO_2?, Front. Ecol. Environ., 2(7), 348–353, doi:10.1890/1540-9295, 2004.

Andersson, A. J. and Mackenzie, F. T.: Revisiting four scientific debates in ocean acidification research, Biogeosciences, 9(3), 893–905, doi:10.5194/bg-9-893-2012, 2012.

Auger, P. A., Diaz, F., Ulses, C., Estournel, C., Neveux, J., Joux, F., Pujo-Pay, M. and Naudin, J. J.: Functioning of the planktonic ecosystem on the Gulf of Lions shelf (NW Mediterranean) during spring and its impact on the carbon deposition: a field data and 3-D modelling combined approach, Biogeosciences, 8(11), 3231–3261, doi:10.5194/bg-8-3231-2011, 2011.

Baklouti, M., Faure, V, Pawlowski, L. and Sciandra, A.: Investigation and sensitivity analysis of a mechanistic phytoplankton model implemented in a new modular numerical tool (Eco3M) dedicated to biogeochemical modelling. Prog. Oceanogr., 71(1), 34-58, doi:10.1016/j.pocean.2006.05.003, 2006.

Borges, A. V and Abril, G.: Carbon ~~Dioxide~~dioxide and ~~Methane Dynamics~~methane dynamics in ~~Estuaries~~estuaries, in Treatise on Estuarine and Coastal Science, edited by E. Wolanski and D. McLusky, pp. 119–161, Academic Press, Waltham., 2011.

Le Borgne, R.: Zooplankton production in the eastern tropical Atlantic Ocean: Net growth efficiency and P:B in terms of carbon, nitrogen, and phosphorus, Limnol. Oceanogr., 27(4), 681–698, doi:10.4319/lo.1982.27.4.0681, 1982.

Le Borgne, R. and Rodier, M.: Net zooplankton and the biological pump: a comparison between the oligotrophic and mesotrophic equatorial Pacific, Deep Sea Res. Part II ~~Top. Stud. Oceanogr.~~, 44(9), 2003–2023, doi:10.1016/S0967-0645(97)00034-9, 1997.

Cai, W.-J.: Estuarine and ~~Coastal Ocean Carbon Paradox~~coastal ocean carbon paradox: CO_2 ~~Sinks~~sinks or ~~Sites~~sites of ~~Terrestrial Carbon Incineration~~terrestrial carbon incineration?, Ann. Rev. Mar. Sci., 3(1), 123–145, doi:10.1146/annurev-marine-120709-142723, 2011.

Cai, W.-J., Hu, X., Huang, W.-J., Murrell, M. C., Lehrter, J. C., Lohrenz, S. E., Chou, W.-C., Zhai, W., Hollibaugh, J. T., Wang, Y., Zhao, P., Guo, X., Gundersen, K., Dai, M. and Gong, G.-C.: Acidification of subsurface coastal waters enhanced by eutrophication, Nat. Geosci., 4(11), 766–770, doi:10.1038/ngeo1297, 2011.

Campbell, R., Diaz, F., Hu, Z., Doglioli, A., Petrenko, A. and Dekeyser, I.: Nutrients and plankton spatial distributions induced by a coastal eddy in the Gulf of Lion. Insights from a numerical model, Prog. Oceanogr., 109, 47–69, doi:10.1016/j.pocean.2012.09.005, 2013.

De Carlo, E. H., Mousseau, L., Passafiume, O., Drupp, P. S. and Gattuso, J.-P.: Carbonate Chemistry and Air–Sea CO_2 Flux in a NW Mediterranean Bay Over a Four-Year Period: 2007–2011, Aquat. Geochemistry, 19(5–6), 399–442, doi:10.1007/s10498-013-9217-4, 2013.

Chen, C.-T. A. and Borges, A. V: Deep-Sea Research II Reconciling opposing views on carbon cycling in the coastal ocean~~:~~ : Continental shelves as sinks and near-shore ecosystems as sources of atmospheric CO_2, Deep Sea Res. II, 56, 578–590, doi:10.1016/j.dsr2.2009.01.001, 2009.

Chen, C.-T. A., Huang, T.-H., Chen, Y.-C., Bai, Y., He, X. and Kang, Y.: Air–sea exchanges of CO_2 in the world's coastal seas, Biogeosciences, 10(10), 6509–6544, doi:10.5194/bg-10-6509-2013, 2013.

Cloern, J. E.: Our evolving conceptual model of the coastal eutrophication problem, Mar. Ecol. Prog. Ser., 210, 223–253, doi:10.3354/meps210223, 2001.

Cloern, J. E., Foster, S. Q. and Kleckner, A. E.: Phytoplankton primary production in the world's estuarine-coastal ecosystems, Biogeosciences, 11, 2477–2501, doi:10.5194/bg-11-2477-2014, 2014.

Cocco, V., Joos, F., Steinacher, M., Frölicher, T. L., Bopp, L., Dunne, J., Gehlen, M., Heinze, C., Orr, J., Oschlies, A., Schneider, B., Segschneider, J. and Tjiputra, J.: Oxygen and indicators of stress for marine life in multi-model global warming projections, Biogeosciences, 10(3), 1849–1868, doi:10.5194/bg-10-1849-2013, 2013.

Copin-Montégut, C., Bégovic, M. and Merlivat, L.: Variability of the partial pressure of CO_2 on diel to annual time scales in the Northwestern Mediterranean Sea, Mar. Chem., 85(3), 169–189, doi:10.1016/j.marchem.2003.10.005, 2004.

Dickson, A. G.: Standard potential of the reaction: $AgCl_{(s)} + 12H_{2(g)} = Ag_{(s)} + HCl_{(aq)}$, and and the standard acidity constant of the ion HSO_4^- in synthetic sea water from 273.15 to 318.15 K, J. Chem. Thermodyn., 22(2), 113–127, doi:10.1016/0021-9614(90)90074-Z, 1990a.

Dickson, A. G.: Thermodynamics of the dissociation of boric acid in synthetic seawater from 273.15 to 318.15 K, Deep Sea Res. ~~Part A. Oceanogr. Res. Pap.~~, 37(5), 755–766, doi:10.1016/0198-0149(90)90004-F, 1990b.

Dickson, A. G. and Riley, J. P.: The estimation of acid dissociation constants in sea-water media from potentiometric titrations with strong base. II. The dissociation of phosphoric acid, Mar. Chem., 7(2), 101–109, doi:10.1016/0304-

Mis en forme : Centré

14

545 4203(79)90002-1, 1979.

546 Doney, S. C., Tilbrook, B., Roy, S., Metzl, N., Le Quéré, C., Hood, M., Feely, R. a. and Bakker, D.: Surface-ocean
547 CO_2 variability and vulnerability, Deep Sea Res. Part II ~~Top. Stud. Oceanogr.~~, 56(8–10), 504–511,
548 doi:10.1016/j.dsr2.2008.12.016, 2009.

549 Esbaugh, A. J., Heuer, R. and Grosell, M.: Impacts of ocean acidification on respiratory gas exchange and acid—base
550 balance in a marine teleost, Opsanus beta, J. Comp. Physiol. B, 182(7), 921–934, doi:10.1007/s00360-012-0668-5,
551 2012.

552 Faure, V., Pinazo, C., Torréton, J.-P. and Jacquet, S.: Modelling the spatial and temporal variability of the SW lagoon
553 of New Caledonia I: A new biogeochemical model based on microbial loop recycling, Mar. Pollut. Bull., 61(7), 465–
554 479, doi:10.1016/j.marpolbul.2010.06.041, 2010.

555 Fraysse, M., Pinazo, C., Faure, V., Fuchs, R., Lazzari, P., Raimbault, P. and Pairaud, I.: Development of a 3D ~~Coupled~~
556 ~~Physical-Biogeochemical Model~~coupled physical-biogeochemical model for the Marseille ~~Coastal Area~~coastal area
557 (NW Mediterranean Sea): What ~~Complexity Is Required~~complexity is required in the Coastal Zone?, PLoS One, 8(12),
558 1–18, doi:10.1371/journal.pone.0080012, 2013.

559 Fraysse, M., Pairaud, I., Ross, O. N., Faure, V. and Pinazo, C.: Intrusion of ~~Rhone~~Rhône River diluted water into the
560 Bay of Marseille: Generation processes and impacts on ecosystem functioning, J. Geophys. Res. Ocean., 119(10),
561 6535–6556, doi:10.1002/2014JC010022, 2014.

562 Fukuda, R., Ogawa, H., Nagata, T. and Koike, I.: Direct Determination of Carbon and Nitrogen Contents of Natural
563 Bacterial Assemblages in Marine Environments, Appl. Environ. Microbiol., 64(9), 3352–3358 [online] Available
564 from: https://aem.asm.org/content/64/9/3352, 1998.

565 Gatti, J., Petrenko, A., Devenon, J.-L., Leredde, Y. and Ulses, C.: The ~~Rhone~~Rhône river dilution zone present in the
566 northeastern shelf of the Gulf of Lion in December 2003, Cont. Shelf Res., 26(15), 1794–1805,
567 doi:10.1016/j.csr.2006.05.012, 2006.

568 Gattuso, J.-P., Frankignoulle, M. and Wollast, R.: Carbon and carbonate metabolism in coastal aquatic ecosystems,
569 Annu. Rev. Ecol. Syst., 29(1), 405–34, doi:10.1146/annurev.ecolsys.29.1.405, 1998.

570 Gattuso, J.-P., Magnan, A., Bille, R., Cheung, W. W. L., Howes, E. L., Joos, F., Allemand, D., Bopp, L., Cooley, S.
571 R., Eakin, C. M., Hoegh-Guldberg, O., Kelly, R. P., Portner, H.-O., Rogers, A. D., Baxter, J. M., Laffoley, D., Osborn,
572 D., Rankovic, A., Rochette, J., Sumaila, U. R., Treyer, S. and Turley, C.: Contrasting futures for ocean and society
573 from different anthropogenic CO_2 emissions scenarios, Science, 349(6243), pp.aac4722, doi:10.1126/science.aac4722,
574 2015.

575 Gehlen, M., Gangstø, R., Schneider, B., Bopp, L., Aumont, O. and Ethe, C.: The fate of pelagic $CaCO_3$ production in
576 a high CO_2 ocean: a model study, Biogeosciences, 4(4), 505–519, doi:10.5194/bg-4-505-2007, 2007.

577 Gemayel, E., Hassoun, A. E. R., Benallal, M. A., Goyet, C., Rivaro, P., Abboud-Abi Saab, M., Krasakopoulou, E.,
578 Touratier, F. and Ziveri, P.: Climatological variations of total alkalinity and total dissolved inorganic carbon in the
579 Mediterranean Sea surface waters, Earth Syst. Dyn., 6(2), 789–800, doi:10.5194/esd-6-789-2015, 2015.

580 Gerber, R. P. and Gerber, M. B.: Ingestion of natural particulate organic matter and subsequent assimilation, respiration
581 and growth by tropical lagoon zooplankton, Mar. Biol., 52(1), 33–43, doi:10.1007/BF00386855, 1979.

582 Gouze, E., Raimbault, P., Garcia, N. and Picon, P.: Nutrient dynamics and primary production in the eutrophic Berre
583 Lagoon (Mediterranean , France), Transitional Waters Bull., 2, 17–40, doi:10.1285/i18252273v2n2p17, 2008.

584 Gruber, N., Clement, D., Carter, B. R., Feely, R. A., van Heuven, S., Hoppema, M., Ishii, M., Key, R. M., Kozyr, A.,
585 Lauvset, S. K., Lo Monaco, C., Mathis, J. T., Murata, A., Olsen, A., Perez, F. F., Sabine, C. L., Tanhua, T. and
586 Wanninkhof, R. H.: The oceanic sink for anthropogenic CO_2 from 1994 to 2007, Science, 363(6432), 1193–1199,
587 doi:10.1126/science.aau5153, 2019.

588 Gutiérrez-Rodríguez, A., Latasa, M., Scharek, R., Massana, R., Vila, G. and Gasol, J. M.: Growth and grazing rate
589 dynamics of major phytoplankton groups in an oligotrophic coastal site, Estuar. Coast. Shelf Sci., 95(1), 77–87,
590 doi:10.1016/j.ecss.2011.08.008, 2011.

591 Harrison, W. G., Harris, L. R. and Irwin, B. D.: The kinetics of nitrogen utilization in the oceanic mixed layer: Nitrate
592 and ammonium interactions at nanomolar concentrations, Limnol. Oceanogr., 41(1), 16–32,
593 doi:10.4319/lo.1996.41.1.0016, 1996.

594 Herrmann, M., Somot, S., Calmanti, S., Dubois, C., and Sevault F.: Representation of spatial and temporal variability
595 of daily wind speed and of intense wind events over the Mediterranean Sea using dynamical downscaling: Impact of
596 the regional climate model configuration, Nat. Hazards Earth Syst. Sci., 11, 1983–2001, doi:10.5194/nhess-11-1983-
597 2011, 2011.

598 Hoegh-Guldberg, O., Jacob, D., Taylor, M., Bindi, M., Brown, S., Camilloni, I., Diedhiou, A., Djalante, R., Ebi, K.,
599 Engelbrecht, F., Guiot, J., Hijioka, Y., Mehrotra, S., Payne, A., Seneviratne, S. I., Thomas, A., Warren, R. and Zhou,
600 G.: Impacts of 1.5°C Global Warming on Natural and Human Systems, in Global warming of 1.5°C. An IPCC Special
601 Report on the impacts of global warming of 1.5°C above pre-industrial levels and related global greenhouse gas
602 emission pathways, in the context of strengthening the global response to the threat of climate change, edited by V.
603 Masson-Delmotte, P. Zhai, H. O. Pörtner, D. Roberts, J. Skea, P. R. Shukla, A. Pirani, W. Moufouma-Okia, C. Péan,
604 R. Pidcock, S. Connors, J. B. R. Matthews, Y. Chen, X. Zhou, M. I. Gomis, E. Lonnoy, T. Maycock, M. Tignor, and

Mis en forme : Centré

605 T. Waterfield, World Meteorological Organization Technical Document., 2018.

606 Kapsenberg, L., Alliouane, S., Gazeau, F., Mousseau, L. and Gattuso, J.-P.: Coastal ocean acidification and increasing
607 total alkalinity in the northwestern Mediterranean Sea, Ocean Sci., 13(3), 411–426, doi:10.5194/os-13-411-2017, 2017.

608 Lacroix, G. and Grégoire, M.: Revisited ecosystem model (MODECOGeL) of the Ligurian Sea: seasonal and
609 interannual variability due to atmospheric forcing, J. Mar. Syst., 37(4), 229–258, doi:10.1016/S0924-7963(02)00190-
610 2, 2002.

611 Leblanc, K., Quéguiner, B., Diaz, F., Cornet, V., Michel-Rodriguez, M., Durrieu de Madron, X., Bowler, C., Malviya,
612 S., Thyssen, M., Grégori, G., Rembauville, M., Grosso, O., Poulain, J., de Vargas, C., Pujo-Pay, M. and Conan, P.:
613 Nanoplanktonic diatoms are globally overlooked but play a role in spring blooms and carbon export, Nat. Commun.,
614 9(1), 953, doi:10.1038/s41467-018-03376-9, 2018.

615 Lueker, T. J., Dickson, A. G. and Keeling, C. D.: Ocean pCO$_2$ calculated from dissolved inorganic carbon, alkalinity,
616 and equations for K1 and K2: Validation based on laboratory measurements of CO$_2$ in gas and seawater at equilibrium,
617 Mar. Chem., 70(June 2015), 105–119, doi:10.1016/S0304-4203(00)00022-0, 2000.

618 Margalef, R.: Life-forms of phytoplankton as survival alternatives in an unstable environment, edited by Gauthier-
619 Villars, Oceanol. Acta, 1(4), 493–509 [online] Available from: https://archimer.ifremer.fr/doc/00123/23403/, 1978.

620 Marty, J.-C., Chiavérini, J., Pizay, M.-D. and Avril, B.: Seasonal and interannual dynamics of nutrients and
621 phytoplankton pigments in the western Mediterranean Sea at the DYFAMED time-series station (1991–1999), Deep
622 Sea Res. Part II Top. Stud. Oceanogr., 49(11), 1965–1985, doi:10.1016/S0967-0645(02)00022-X, 2002.

623 Matthews, H. D., Gillett, N. P., Stott, P. a and Zickfeld, K.: The proportionality of global warming to cumulative
624 carbon emissions., Nature, 459(7248), 829–32, doi:10.1038/nature08047, 2009.

625 Mella-Flores, D., Mazard, S., Humily, F., Partensky, F., Mahé, F., Bariat, L., Courties, C., Marie, D., Ras, J., Mauriac,
626 R., Jeanthon, C., Mahdi Bendif, E., Ostrowski, M., Scanlan, D. J. and Garczarek, L.: Is the distribution of
627 Prochlorococcus and Synechococcus ecotypes in the Mediterranean Sea affected by global warming?, Biogeosciences,
628 8(9), 2785–2804, doi:10.5194/bg-8-2785-2011, 2011.

629 Middelburg, J. J.: Marine ~~Carbon Biogeochemistry A Primer~~carbon biogeochemistry a primer for ~~Earth System~~
630 ~~Scientists~~earth system scientists, Springer B., edited by Springer Briefs in Earth System Sciences, Springer Briefs in
631 Earth System Sciences, 2019.

632 Millero, F. J.: Thermodynamics Seawater - 1. The PVT Properties, *Ocean Science and Engineering*, 7(4), 403-460
633 1982.

634 Millero, F. J.: Thermodynamics of the carbon dioxide system in the oceans, Geochim. Cosmochim. Acta, 59(4), 661–
635 677, doi:10.1016/0016-7037(94)00354-O, 1995.

636 Millet, B., Pinazo, C., Daniela, B., Remi, P., Pierre, G. and Ivane, P.: Unexpected spatial impact of treatment plant
637 discharges induced by episodic hydrodynamic events: Modelling Lagrangian transport of fine particles by Northern
638 Current intrusions in the bays of Marseille (France), edited by P. L. Science, PLoS One, 13(4), e0195257 (25p.),
639 doi:10.1371/journal.pone.0195257, 2018.

640 Millot, C.: The Gulf of Lions hydrodynamics, Cont. Shelf Res., 10(9), 885–894, doi:10.1016/0278-4343(90)90065-T,
641 1990.

642 Monterey, G. and Levitus, S.: Seasonal ~~Variability~~variability of ~~Mixed Layer Depth~~mixed layer depth for the World
643 Ocean, NOAA Atlas NESDIS 14, Washington, D. C., 1997.

644 Moran, M. A.: The global ocean microbiome, Sci. Am. Assoc. Adv. Sci., 350(6266), doi:10.1126/science.aac8455,
645 2015.

646 Morris, A. W. and Riley, J. P.: The bromide/chlorinity and sulphate/chlorinity ratio in sea water, Deep Sea Res.
647 Oceanogr. Abstr., 13(4), 699–705, doi:10.1016/0011-7471(66)90601-2, 1966.

648 Mucci, A.: The solubility of calcite and aragonite in seawater at various salinities, temperatures, and one atmosphere
649 total pressure, Am. J. Sci., 283(7), 780–799, doi:10.2475/ajs.283.7.780, 1983.

650 Orr, J. C., Fabry, V. J., Aumont, O., Bopp, L., Doney, S. C., Feely, R. A., Gnanadesikan, A., Gruber, N., Ishida, A.,
651 Joos, F., Key, R. M., Lindsay, K., Maier-Reimer, E., Matear, R., Monfray, P., Mouchet, A., Najjar, R. G., Plattner, G.-
652 K., Rodgers, K. B., Sabine, C. L., Sarmiento, J. L., Schlitzer, R., Slater, R. D., Totterdell, I. J., Weirig, M.-F.,
653 Yamanaka, Y. and Yool, A.: Anthropogenic ocean acidification over the twenty-first century and its impact on
654 calcifying organisms, Nature, 437(7059), 681–6, doi:10.1038/nature04095, 2005.

655 Pairaud, I., Gatti, J., Bensoussan, N., Verney, R. and Garreau, P.: Hydrology and circulation in a coastal area off
656 Marseille: Validation of a nested 3D model with observations, J. Mar. Syst., 88(1), 20–33,
657 doi:10.1016/j.jmarsys.2011.02.010, 2011.

658 Para, J., Coble, P. G., Charrière, B., Tedetti, M., Fontana, C. and Sempéré, R.: Fluorescence and absorption properties
659 of chromophoric dissolved organic matter (CDOM) in coastal surface waters of the northwestern Mediterranean Sea,
660 influence of the Rhône River, Biogeosciences, 7(12), 4083–4103, doi:10.5194/bg-7-4083-2010, 2010.

661 Petrenko, A.: Variability of circulation features in the Gulf of Lion, NW Mediterranean Sea . Importance of inertial
662 currents ~~Variabilité de la circulation dans le golfe du Lion (Méditerranée nord-occidentale). Importance des courants~~
663 ~~d ' inertie.~~, Oceanol. Acta, 26, 323–338, doi:10.1016/S0399-1784(03)00038-0, 2003.

Mis en forme : Centré

16

664 Pont, D., Simonnet, J.-P. and Walter, A. V~~.~~: Medium-term ~~Changes~~changes in ~~Suspended Sediment~~
665 ~~Delivery~~suspended sediment delivery to the Ocean: Consequences of ~~Catchment Heterogeneity~~catchment
666 heterogeneity and ~~River Management~~river management (Rhône River, France), Estuar. Coast. Shelf Sci., 54(1), 1–18,
667 doi:10.1006/ecss.2001.0829, 2002.

668 Le Quéré, C., Andrew, R. M., Friedlingstein, P., Sitch, S., Hauck, J., Pongratz, J., Pickers, P. A., Korsbakken, J. I.,
669 Peters, G. P., Canadell, J. G., Arneth, A., Arora, V. K., Barbero, L., Bastos, A., Bopp, L., Chevallier, F., Chini, L. P.,
670 Ciais, P., Doney, S. C., Gkritzalis, T., Goll, D. S., Harris, I., Haverd, V., Hoffman, F. M., Hoppema, M., Houghton, R.
671 A., Hurtt, G., Ilyina, T., Jain, A. K., Johannessen, T., Jones, C. D., Kato, E., Keeling, R. F., Goldewijk, K. K.,
672 Landschützer, P., Lefèvre, N., Lienert, S., Liu, Z., Lombardozzi, D., Metzl, N., Munro, D. R., Nabel, J. E. M. S.,
673 Nakaoka, S.-I., Neill, C., Olsen, A., Ono, T., Patra, P., Peregon, A., Peters, W., Peylin, P., Pfeil, B., Pierrot, D., Poulter,
674 B., Rehder, G., Resplandy, L., Robertson, E., Rocher, M., Rödenbeck, C., Schuster, U., Schwinger, J., Séférian, R.,
675 Skjelvan, I., Steinhoff, T., Sutton, A., Tans, P. P., Tian, H., Tilbrook, B., Tubiello, F. N., van der Laan-Luijkx, I. T.,
676 van der Werf, G. R., Viovy, N., Walker, A. P., Wiltshire, A. J., Wright, R., Zaehle, S. and Zheng, B.: Global Carbon
677 Budget 2018, Earth Syst. Sci. Data, 10(4), 2141–2194, doi:10.5194/essd-10-2141-2018, 2018.

678 Raven, J. A. and Falkowski, P. G.: Oceanic sinks for atmospheric CO_2, Plant. Cell Environ., 22(6), 741–755,
679 doi:10.1046/j.1365-3040.1999.00419.x, 1999.

680 Riley, J. P.: The occurrence of anomalously high fluoride concentrations in the North Atlantic, Deep Sea Res.
681 Oceanogr. Abstr., 12(2), 219–220, doi:10.1016/0011-7471(65)90027-6, 1965.

682 Riley, J. P. and Tongudai, M.: The major cation/chlorinity ratios in sea water, Chem. Geol., 2, 263–269,
683 doi:10.1016/0009-2541(67)90026-5, 1967.

684 Roobaert, A., Laruelle, G. G., Landschützer, P., Gruber, N., Chou, L. and Regnier, P.: The ~~Spatiotemporal~~
685 ~~Dynamics~~spatiotemporal dynamics of the ~~Sources~~sources and ~~Sinks~~sinks of CO_2 in the ~~Global Coastal Ocean~~global
686 coastal ocean, Global Biogeochem. Cycles, 33, doi:10.1029/2019GB006239, 2019.

687 Ross, O. N., Fraysse, M., Pinazo, C. and Pairaud, I.: Impact of an intrusion by the Northern Current on the
688 biogeochemistry in the eastern Gulf of Lion, NW Mediterranean, Estuar. Coast. Shelf Sci., 170, 1–9,
689 doi:10.1016/j.ecss.2015.12.022, 2016.

690 Rykiel, E. J.: Testing ecological models: The meaning of validation, Ecol. Modell., 90(3), 229–244, doi:10.1016/0304-
691 3800(95)00152-2, 1996.

692 Sarthou, G., Timmermans, K. R., Blain, S. and Tréguer, P.: Growth physiology and fate of diatoms in the ocean: a
693 review, J. Sea Res., 53(1), 25–42, doi:10.1016/j.seares.2004.01.007, 2005.

694 Schneider, A., Wallace, D. W. R. and Körtzinger, A.: Alkalinity of the Mediterranean Sea, Geophys. Res. Lett., 34(15),
695 doi:10.1029/2006GL028842, 2007.

696 Sempéré, R., Charrière, B., van Wambeke, F., and Cauwet, G.: Carbon inputs of the Rhône River to the Mediterranean
697 Sea: Biogeochemical implications, Global Biogeochem. Cycles, 14(2), 669-681, doi:10.1029/1999GB900069, 2000.

698 Small, C. and Nicholls, R. J.: A ~~Global Analysis of Human Settlement~~global analysis of human settlement in ~~Coastal~~
699 ~~Zones~~coastal zones, J. Coast. Res., 19(3), 584–599 [online] Available from: http://www.jstor.org/stable/4299200,
700 2003.

701 Smith, C. L. and Tett, P.: A depth-resolving numerical model of physically forced microbiology at the European shelf
702 edge, J. Mar. Syst., 26(1), 1–36, doi:10.1016/S0924-7963(00)00010-5, 2000.

703 Soetaert, K., Hofmann, A. F., Middelburg, J. J., Meysman, F. J. R. and Greenwood, J.: The effect of biogeochemical
704 processes on pH, Mar. Chem., 105(1–2), 30–51, doi:10.1016/j.marchem.2006.12.012, 2007.

705 Tett, P.: A three-layer vertical and microbiological processes model for shelf seas., 1990.

706 Tett, P., Droop, M. R. and Heaney, S. I.: The Redfield ~~Ratio~~ratio and ~~Phytoplankton Growth Rate~~phytoplankton growth
707 rate, J. Mar. Biol. Assoc. United Kingdom, 65(2), 487–504, doi:10.1017/S0025315400050566, 1985.

708 Thingstad, T. F.: Utilization of N, P, and organic C by heterotrophic bacteria . I. Outline of a chemostat theory with a
709 consistent concept of "maintenance" metabolism, Mar. Ecol. Prog. Ser., 35, 99–109, doi:10.3354/meps035099, 1987.

710 Uppström, L. R.: The boron/chlorinity ratio of deep-sea water from the Pacific Ocean, Deep Sea Res. Oceanogr. Abstr.,
711 21(2), 161–162, doi:10.1016/0011-7471(74)90074-6, 1974.

712 Upstill-Goddard, R. C.: Air-sea gas exchange in the coastal zone, Estuar. Coast. Shelf Sci., 70(3), 388–404,
713 doi:10.1016/j.ecss.2006.05.043, 2006.

714 Wanninkhof, R. H.: Relationship ~~Between Wind Speed~~between wind speed and ~~Gas Exchange~~gas exchange, J.
715 Geophys. Res., 97(C5), 7373–7382, 1992.

716 Weiss, R. F.: Carbon dioxide in water and seawater: the solubility of a non-ideal gas, Mar. Chem., 2(3), 203–215,
717 doi:10.1016/0304-4203(74)90015-2, 1974.

718 Willmott, C. J.: Some comments on the evaluation of model performance, Bull. Am. Meteorol. Soc., 63(11), 1982.

719 Wimart-Rousseau, C., Lajaunie-Salla, K., Marrec, P., Wagener, T., Raimbault, P., Lagadec, V., Lafont, M., Garcia,
720 N., Diaz, F., Pinazo, C., Yohia, C., Garcia, F., Xueref-Remy, I., Blanc, P. E., Armengaud, A. and Lefèvre, D.: Temporal
721 variability of the carbonate system and air-sea CO_2 exchanges in a Mediterranean human-impacted coastal site, Estuar.
722 Coast. Shelf Sci., 236(February), doi:10.1016/j.ecss.2020.106641, 2020.

723 Xueref-Remy, I., Milne, M., Zoghbi, N., Yohia, C., Armengaud, A., Blanc, P.-E., Delmotte, M., Piazzola, J., Nathan,
724 B., Ramonet, M. and Lac, C.: Assessing atmospheric CO_2 variability in the Aix-Marseille metropolis area (France)
725 and its coastal Mediterranean Sea at different time scales within the AMC project, Prague, Aus, [online] Available
726 from: https://conference.icos-ri.eu/wp-ontent/uploads/2018/09/ICOS2018SC_Book_of_Abstracts.pdf, 2018a.

727 Xueref-Remy, I., Dieudonné, E., Vuillemin, C., Lopez, M., Lac, C., Schmidt, M., Delmotte, M., Chevallier, F., Ravetta,
728 F., Perrussel, O., Ciais, P., Bréon, F., Broquet, G., Ramonet, M. and Ampe, C.: Diurnal , synoptic and seasonal
729 variability of atmospheric CO_2 in the Paris megacity area, Atmos. Chem. Phys., 18, 3335–3362, doi:10.5194/acp-18-
730 3335-2018, 2018b.

731 Yohia, C.: Genèse du mistral par interaction barocline et advection du tourbillon potentiel, Climatologie, 13, 24–37
732 [online] Available from: https://doi.org/10.4267/climatologie.1182, 2017.

733 Zappa, C. J., Raymond, P. A., Terray, E. A. and McGillis, W. R.: Variation in ~~Surface Turbulence~~surface turbulence
734 and the ~~Gas Transfer Velocity~~gas transfer velocity over a ~~Tidal Cycle~~tidal cycle in a ~~Macro~~macro-tidal ~~Estuary~~estuary,
735 Estuaries, 26(6), 1401–1415, 2003.

736
737

Mis en forme : Centré

18

Tables

	Temperature	Wind	River input	Atmospheric CO₂
S0 – Reference	In situ data of 2017	WRF model 2017	No	CAV station 2017
S1 - T increases	In situ data of 2017 +1.5°C	WRF model 2017	No	CAV station 2017
S2 - Wind constant	In situ data of 2017	7 m s⁻¹	No	CAV station 2017
S3 - Wind events	In situ data of 2017	3 days ~~of~~at 20 m s⁻¹	No	CAV station 2017
S4 - NO₃	In situ data of 2017	WRF model 2017	Yes, NO₃ ~~inputs~~	CAV station 2017
~~**S5 - TA**~~	~~In situ data of 2017~~	~~WRF model 2017~~	~~TA inputs~~	~~CAV station 2017~~
~~**S6**~~**S5 - Non-urban**	In situ data of 2017	WRF model 2017	No	OHP station 2017

Table 1: Forcing of the different scenarios (S) simulated with the model. See section 2.4 for details of scenarios.

	Chl	seawater pCO₂	pH	DIC	TA
Obs min-max	[0.10– 1.71]	[358 – 471]	[8.014 – 8.114]	[2260 – 2348]	[2561 – 2624]
Mod min-max	[0.03 – 0.73]	[331 – 522]	[7.979 – 8.171]	[2220 – 2323]	[2560– 2572]
Bias	-0.22	22.47	-0.016	-8.48	-24.91
WSS	0.36	0.69*	0.75*	0.71*	0.43
N	22	20	21	20	20

Table 2: Statistical evaluation of observations *vs*. model for 2017 year: observed and simulated minimum and maximum values, WSS = Wilmott Skill Score, N = number of measurements. Units of bias are those of modeled variables: chlorophyll *a* (Chl, mg m⁻³), seawater pressure of CO₂ (seawater *p*CO₂, μatm), *p*H, dissolved inorganic carbon (DIC, μmol kg⁻¹) and total alkalinity (TA, μmol kg⁻¹)~~ .~~). *significant value of WSS (> 0.70).

Mis en forme : Police :Italique

		Aeration	GPP	R$_A$	R$_H$	R	NEP
Mean flux	**Year**	0.017	-0.413	0.065	0.348	0.413	0
	MWC	-0.245	-0.314	0.052	0.176	0.228	0.086
	SWC	0.405	-0.521	0.079	0.555	0.634	-0.113
Contribution	**Year**	78%	11%	2%	9%	11%	~~/~~

Table 3: Mean flux values (mmol m⁻³ d⁻¹) and the contribution of each process to the DIC variations for the reference simulation over the year and SWC/MWC periods. GPP: Gross primary production, R$_A$: Autotroph respiration, R$_H$: heterotroph respiration, NEP: Net Ecosystem Production

Mis en forme : Centré

749   **Figures**

750
751
752   **Figure 1: Schematic diagram of the biogeochemical model Eco3M-CarbOx. Explicit state variables of the model are**
753   **indicated in continuous-line box or circles except the implicit variable for zooplankton (dotted line box). Orange-written**
754   **state variables are added variables compared to the preexisting biogeochemical model of Fraysse et al. (2013). Arrows**
755   **represent processes between two state variables. TA: Total Alkalinity. DIC: Dissolved Inorganic Carbon, CO$_2$: carbon**
756   **dioxide, O$_2$: Oxygen, CaCO$_3$: calcium carbonate.**

757
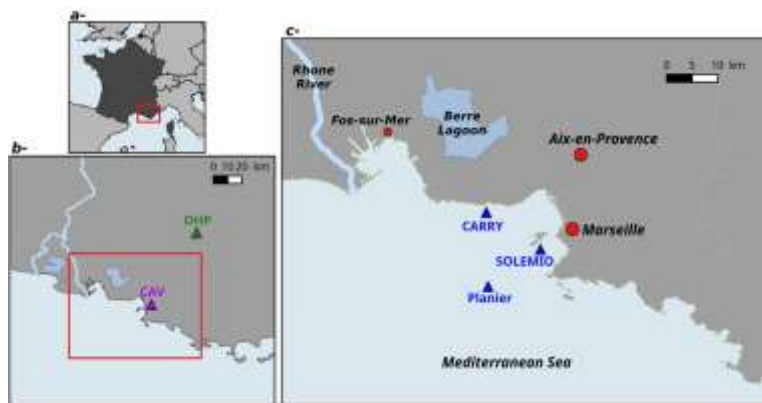
758
759 **Figure 2: Map of study area: The Region Sud (A), Aix-Marseille Metropolis (B), the Bay of Marseille (C). CAV= Cinq**
760 **AVenues Station (urban site), OHP: Observatoire de Haute Provence station (non-urban site), Carry, Solemio, Planier:**
761 ~~Study~~Marine study sites ~~at sea~~ **in the Bay of Marseille.**

762

763
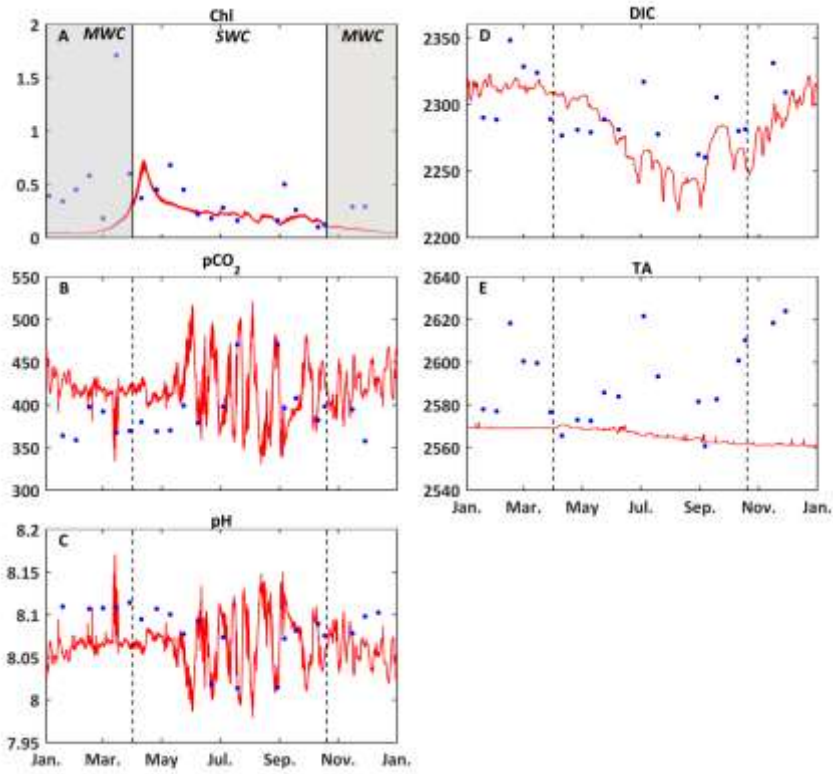
764
765 **Figure 3: Comparison of model results (red) and** *in situ* **data (blue) at the <u>surface of the </u>SOLEMIO station. (A) Chlorophyll-**
766 **a concentrations (mg m^{-3}), (B) pCO$_2$ (µatm), (C) pH, (D) DIC (µmol kg^{-1}), (E) TA (µmol kg^{-1}). The value of each state variable**
767 **represents the mean around ±5 days of the sampling date~~, and the error bars are the standard deviation of values over this~~**
768 **~~time period.~~. The shaded area and dotted black line delimit the SWC and MWC periods.**

769

22
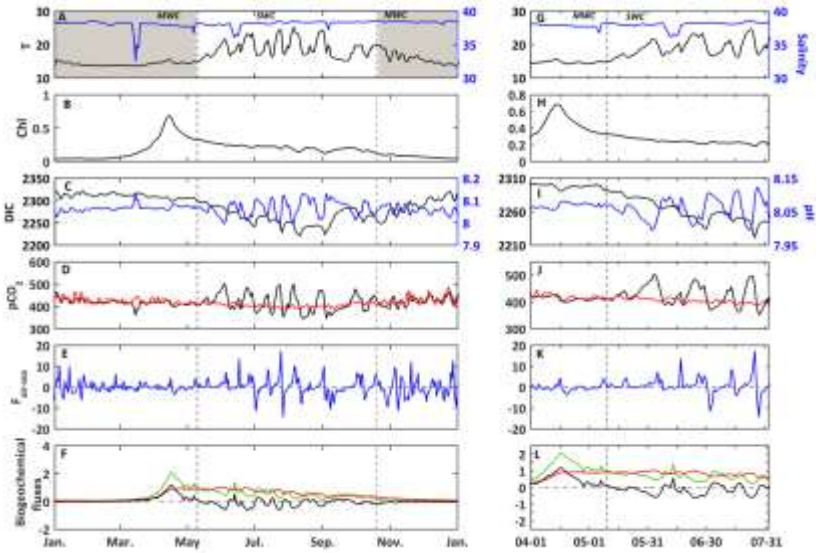
770
771 **Figure 4: In the left panels: year 2017, right panels: temporal focus between April 1st and July 31th, 2017.** *In situ* **daily**
772 **average of (A, G) temperature (°C, black line) and salinity (blue line) at the SOLEMIO station. (at the surface). Modeled**
773 **daily average (B, H) chlorophyll** *a* **concentrations (mg m^{-3}, black line) (C, I) DIC (μmol kg^{-1}, black line) and** *p***H (blue line),**
774 **(D, J) seawater** *p***CO$_2$ (μatm, black line) and atmosphere** *p***CO$_2$ from OHP (μatm, red line), (E, K) air-sea CO$_2$ fluxes mmol**
775 **m^{-3} d^{-1}), (F, L) Gross Primary Production (mmol m^{-3} d^{-1}, green line), total respiration (mmol m^{-3} d^{-1}, red line) and Net**
776 **Ecosystem Production (mmol m^{-3} d^{-1}, black line). The shaded areas and dotted black lines delimit the SWC and MWC**
777 **periods.**

778

Mis en forme : Centré

779
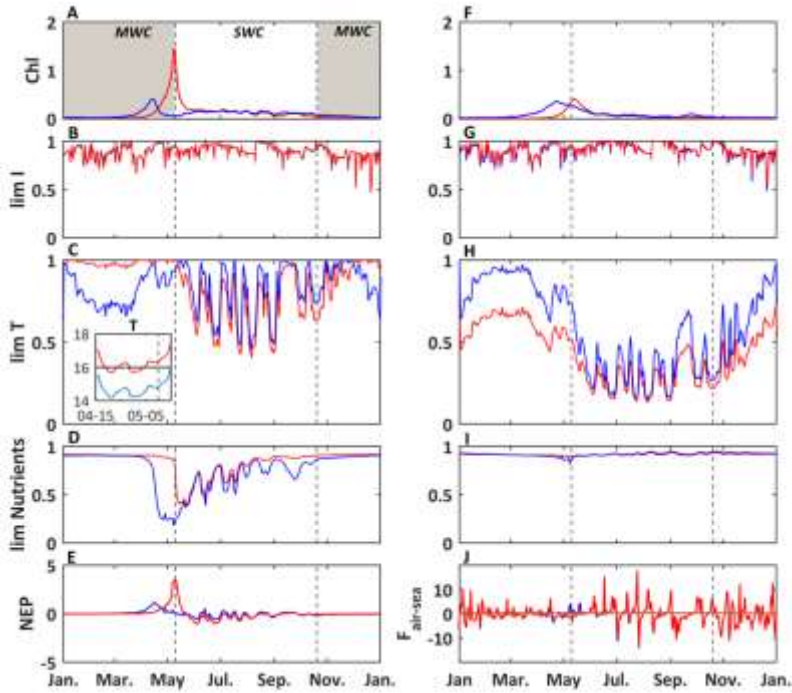
Figure 5: Modeled daily average chlorophyll _a_ concentrations (mg m^{-3}) (A), light limitation (B), temperature limitation, and a zoom from April 15th to May 5th of temperature (C) and nutrient limitation (D) for picophytoplankton and the same set for diatoms (F, G, H and I). Modeled daily average NEP (mmol m^{-3} d^{-1}, E) and air-sea CO$_2$ flux (mmol m^{-3} d^{-1}, J). Reference simulation (S0, blue line) and temperature-shifted simulation by 1.5°C (S2, red line). The shaded area and dotted black lines delimit the SWC and MWC periods.

786
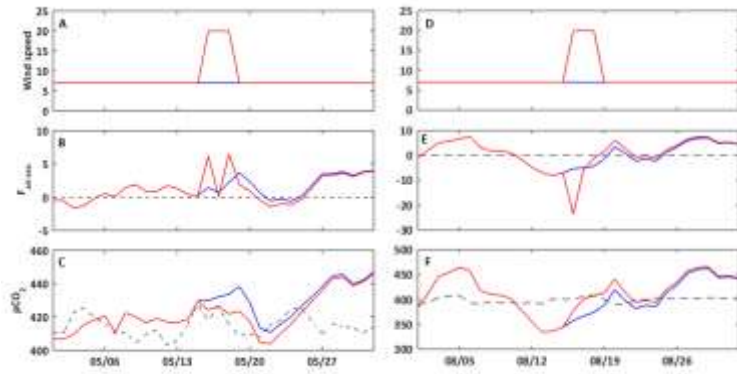
787
Figure 6: Temporal evolution for May (left panels) and August (right panels) 2017 of the wind speed (m s^{-1}, A, D); air-sea
CO$_2$ fluxes (mmol m^{-3} d^{-1}, B, E); seawater partial pressure of CO$_2$ (µatm, C, F). Constant wind scenario (S2, blue line) and
wind event scenario (S3, red line). On panels C and F, the dashed line represents the atmosphere partial pressure of CO$_2$
(µatm) at the CAV station.

792

Mis en forme : Centré
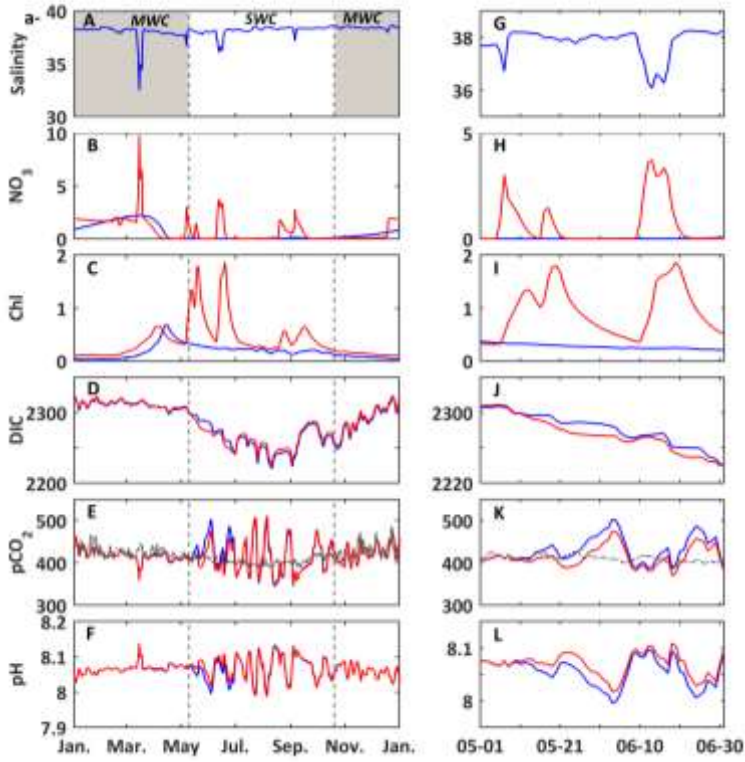
Figure 7: In the left panels: year 2017 and right panels: temporal focus between May 1st and July 1st, 2017. (A, G) *In situ* daily average of salinity. Modeled daily average (B, H) nitrate concentrations (mmol m^{-3}); (C, I) chlorophyll *a* concentrations (mg m^{-3}); (D, J) DIC (µmol kg^{-1}); (E, K) seawater pCO$_2$ (µatm), and (F, L) pH. Reference simulation (S0, blue line) and nitrate supply simulation (S4, red line). On panels E and K, the dashed line represents the atmosphere partial pressure of CO$_2$ (µatm) at the CAV station. The shaded area and dotted black lines delimit the SWC and MWC periods.
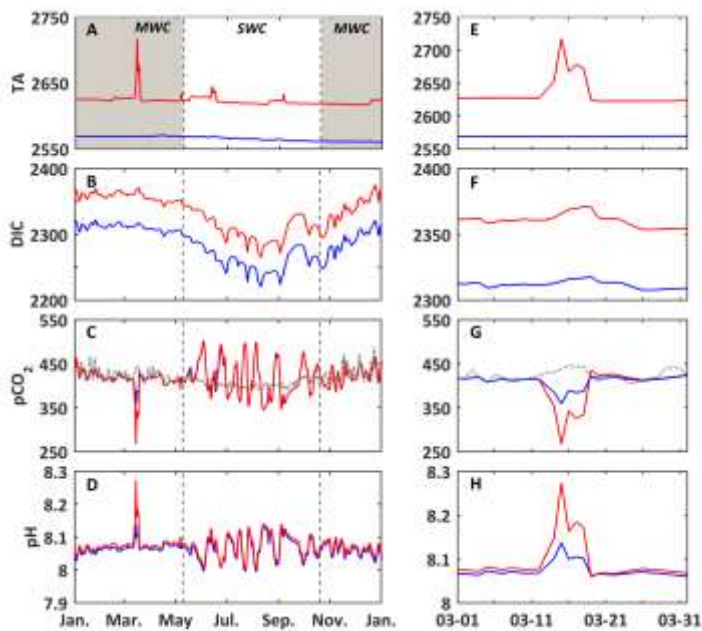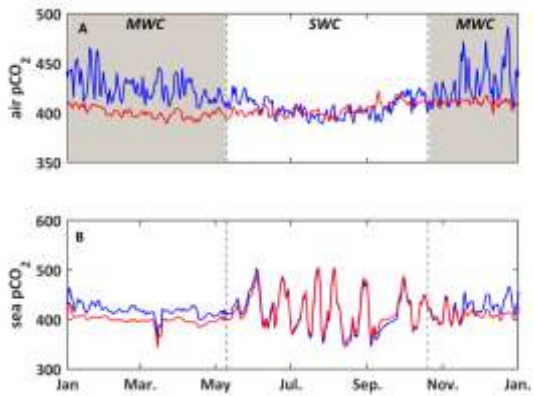
Figure 8: ~~In the left for the whole year 2017 and in the right between March 1ˢᵗ and April 1ˢᵗ, 2017. Modelled daily average~~ (A, E) TA (μmol kg^{-1}); (B, F) DIC (μmol kg^{-1}); (C, G) seawater pCO$_2$ (μatm), and (D, H) pH. Reference simulation (S0, blue line) and alkalinity supply simulation (S5, red line). On the panels C and G, the dashed line represents the atmosphere partial pressure of CO$_2$ (μatm) at the CAV station. The shaded area and dotted black lines delimit the SWC and MWC periods.

810
811 Figure 9: (A) Temporal evolution for the year 2017 of the observed partial pressure of CO_2 (uatm) in the atmosphere in
812 uatm at the CAV station, called the "urban scenario" (S0, blue line), and at the OHP station, called the "non-urban
813 scenario", and in seawater (S6, red line). (B) Temporal evolution for the year 2017 of the modeled seawater partial pressure
814 of CO_2 (µatm) with forcings from the urban (S0, blue line) and non-urban (S6, red line) scenarios. The shaded area and
815 dotted black lines delimit the SWC and MWC periods.

Mis en forme : Centré

Appendix A: Details of resolution of carbonate system module

A.1. Calculation of carbonate systems constants:

- ~~Concentration in~~ Total Fluoride (TF) ~~ions~~concentrations from Riley (1965) in mol kg^{-1}:

$$TF = \frac{0.000067}{18.998} \cdot \frac{S}{1.80655}$$

820
- ~~Concentration in~~ Total Sulphate (TS) ~~ions~~concentration from Morris and Riley (1966) in mol kg^{-1}:

$$TS = \frac{0.14}{96.062} \cdot \frac{S}{1.80655}$$

- Calcium ion concentration from Riley and Tongudai (1967) in mol kg^{-1}:

$$Ca^{2+} = \frac{0.02128}{40.087} \cdot \frac{S}{1.80655}$$

- ~~Concentration in~~ Total Boron (TB) ~~ions~~concentration from Uppström (1974) in mol kg^{-1}:

825 $$TB = \frac{0.000416 \cdot S}{35}$$

- Ionic Strength (IonS) from Millero (1982):

$$IonS = \frac{19.924 \cdot S}{1000 - 1.005 \cdot S}$$

The constants are calculated ~~in~~on the total pH scale except for K$_S$ ~~in~~on free pH scale

830
- If necessary, pH scale conversion factors are following:

From Seawater pH Scale (SWS) to total pH scale: $\text{SWStoTOT} = \dfrac{1 + \frac{TS}{K_S}}{1 + \frac{TS}{K_S} + \frac{TF}{K_F}}$

From Free pH Scale to Total pH scale: $FREEtoTOT = 1 + \dfrac{TS}{K_S}$

- K_S equilibrium constant of dissociation of HSO$_4^-$ from Dickson (1990a) in mol kg^{-1}:

835 $$K_S = \frac{-4276.1}{T_{(K)}} + 141.328 - 23.093 \cdot \log(T_{(K)}) + \left(324.57 - 47.986 \cdot \log(T_{(K)}) - \frac{13856}{T_{(K)}}\right) \cdot Ions^2$$

$$K_S = K_S + \left(-771.54 + 114.723 \cdot \log(T_{(K)}) + \frac{35474}{T_{(K)}}\right) \cdot Ions + \frac{-2698}{T_{(K)}} \cdot \cancel{Ions^{1.5}} + \cancel{\frac{1776}{T_{(K)}}} Ions^{\frac{3}{2}} + \frac{1776}{T_{(K)}} \cdot Ions^2$$

$$K_S = e^{K_S} \cdot (1 - 0.001005 \cdot S)$$

- K_F equilibrium constant of dissociation of hydrogen fluoride ~~ions~~ (HF) formation from Dickson and Riley (1979) in mol kg^{-1}:

840 $$\cancel{K_F = e^{\frac{1590.2}{T_{(K)}} - 12.641 + 1.525 \cdot Ions^{1.5}} \cdot (1 - 0.001005 \cdot S)} K_F = e^{\frac{1590.2}{T_{(K)}} - 12.641 + 1.525 \cdot Ions^{\frac{1}{2}}} \cdot (1 - 0.001005 \cdot S)$$

- K_B equilibrium constant of dissociation of boric acid from Dickson (1990b) in mol kg^{-1}

$$K_B = (-8966.9 - 2890.53 \cdot S^{\frac{1}{2}} - 77.942 \cdot S + 1.728 \cdot S^{\frac{3}{2}} - 0.0996 \cdot S^2)/T_{(K)}$$

$$K_B = K_B + 148.0248 + 137.1942 \cdot S^{\frac{1}{2}} + 1.62142 \cdot S + (-24.4344 - 25.085 \cdot S^{\frac{1}{2}} - 0.2474 \cdot S) \cdot \log(T) + 0.053105 \cdot S^{\frac{1}{2}} \cdot T$$

845   • K_0 constant of CO_2 solubility from Weiss (1974) in mol kg^{-1} atm^{-1}:

$$K_0 = \exp\left(-60.2409 + 93.4517 \cdot \frac{100}{T_{(K)}} + 23.3585 \cdot \log\left(\frac{T_{(K)}}{100}\right) + S \cdot \left(0.023517 - 0.023656 \cdot \frac{T_{(K)}}{100} + 0.0047036 \cdot \left(\frac{T_{(K)}}{100}\right)^2\right)\right)$$

    • K_e: Dissociation constant of water from Millero (1995) in (mol kg^{-1})^2 :

$$K_e = \exp\left(\frac{-13847.26}{T_{(K)}} + 148.9802 - 23.6521 \cdot \log(T_{(K)}) + \left(-5.977 + \frac{118.67}{T_{(K)}} + 1.0495 \cdot \log(T_{(K)})\right) \cdot \cancel{S^{1/2}} S^{\frac{1}{2}} - 0.01615 \cdot S\right)$$

850 $K_e = K_e \cdot SWStoTOT$, ~~in~~on total pH scale in mol kg^{-1}

    • K_1 and K_2 from Lueker et al. (2000) in mol kg^{-1}:

$$K_1 = 10^{\frac{-3633.86}{T_{(K)}} + 61.2172 - 9.6777 \cdot \log(T_{(K)}) + 0.011555 \cdot S - 0.0001152 \cdot S^2}$$

$$K_2 = 10^{\frac{-471.78}{T_{(K)}} + 251.929 - 3.16967 \cdot \log(T_{(K)}) + 0.01781 \cdot S - 0.0001122 \cdot S^2}$$

    • K_{ca} for calcite from Mucci (1983) in (mol kg^{-1})^2:

855 K_{ca}

$= \cancel{10^{-171.9065 - 0.077993 \cdot T_{(K)} + \frac{2839.319}{T_{(K)}} + 71.595 \cdot log10(T_{(K)}) + (-0.77712 + 0.0028426 \cdot T_{(K)} + \frac{178.34}{T_{(K)}}) S^{\frac{1}{2}} - 0.07711 \cdot S + 0.0041249 \cdot S^{1.5}}}$ $10^{-171.9065 - 0.077993 \cdot T_{(K)} + \frac{2839.319}{T_{(K)}} + 71.595 \cdot log10(T_{(K)}) + (-0.77712 + 0.002842 \ldots}$

    • ~~Every constant~~All the constants are corrected by the effect of hydrostatic pressure:

$R = 83.1451$ in ml bar^{-1} K^{-1} mol^{-1}

$$lnK_1fac = \frac{\left(25.5 - 0.1271 \cdot T_{(°C)} + 0.5 \cdot \left(\frac{-3.08 + 0.0877 \cdot T_{(°C)}}{1000}\right) \cdot P_{bar}\right) \cdot P_{bar}}{R * T_{(K)}}; \; K_1 = K_1 \cdot e^{lnK_1fac}$$

860 $$lnK_2fac = \frac{\left(15.82 - 0.0219 \cdot T_{(°C)} + 0.5 \cdot \left(\frac{1.13 + 0.1475 \cdot T_{(°C)}}{1000}\right) \cdot P_{bar}\right) \cdot P_{bar}}{R \cdot T_{(K)}}; \; K_2 = K_2 \cdot e^{lnK_2fac}$$

$$lnK_Bfac = \frac{\left(29.48 - 0.1622 \cdot T_{(°C)} + 0.002608 \cdot T_{(°C)}^2 + 0.5 \cdot \left(\frac{-2.84}{1000}\right) \cdot P_{bar}\right) \cdot P_{bar}}{R \cdot T_{(K)}}; \; K_B = K_B \cdot e^{lnK_Bfac}$$

$$lnK_efac = \frac{\left(20.02 - 0.1119 \cdot T_{(°C)} + 0.001409 \cdot T_{(°C)}^2 + 0.5 \cdot \left(\frac{-5.13 + 0.0794 \cdot T_{(°C)}}{1000}\right) \cdot P_{bar}\right) \cdot P_{bar}}{R \cdot T_{(K)}}; \; K_e = K_e \cdot e^{lnK_efac}$$

$$lnK_Ffac = \frac{\left(9.78 - 0.009 \cdot T_{(°C)} + 0.0009429 \cdot T_{(°C)}^2 + 0.5 \cdot \left(\frac{-3.91 + 0.054 \cdot T_{(°C)}}{1000}\right) \cdot P_{bar}\right) \cdot P_{bar}}{R \cdot T_{(K)}}; \; K_F = K_F \cdot e^{lnK_Ffac}$$

$$lnK_Sfac = \frac{\left(18.03 - 0.0466 \cdot T_{(°C)} + 0.000316 \cdot T_{(°C)}^2 + 0.5 \cdot \left(\frac{-4.53 + 0.009 \cdot T_{(°C)}}{1000}\right) \cdot P_{bar}\right) \cdot P_{bar}}{R \cdot T_{(K)}}; \; K_S = K_S \cdot e^{lnK_Sfac}$$

865 $$lnK_cafac = \frac{\left(48.76 - 0.5304 \cdot T_{(°C)} + 0.5 \cdot \left(\frac{-11.76 + 0.3692 \cdot T_{(°C)}}{1000}\right) \cdot P_{bar}\right) \cdot P_{bar}}{R \cdot T_{(K)}}; \; K_{ca} = K_{ca} \cdot e^{lnK_cafac}$$

    • Calculation of the Fugacity factor:

We suppose that the pressure is at one atmosphere or close to it (Weiss, 1974):

$P_{atm} = 1.01325 \; bar$

$delta = 57.7 - 0.118 \cdot T$ in cm^3 mol^{-1}

870 $b = -1636.75 + 12.0408 \cdot T - 0.0327957 \cdot T^2 + 3.16528 \cdot 0.00001 \cdot T^3$ in cm^3 mol^{-1}

$$FugFac = \exp^{\frac{(b + 2 \cdot delta) \cdot P_{atm}}{R \cdot T}}$$

A.2. Resolution of carbonate system

To resolve the carbonate system, we calculate the $deltapH$, which is the difference of pH between two iterations of the model. We initialize the run by imposing a pH value of 8.

875

$if\ (nbiter < 1)\ pH = 8$

$pHtol = 0.001$! tolerance for iterations end

$deltapH = pHtol + 1$

$do\ while\ (abs(deltapH) > 0.0001)$

880
$\quad H = 10^{-pH}$
$\quad Denom = H^2 + K_1 \cdot H + K_1 \cdot K_2$
$\quad CAlk = DIC \cdot K_1 \cdot \left(\dfrac{H + 2 \cdot K_2}{Denom}\right)$
$\quad BAlk = \dfrac{TB \cdot K_B}{K_B + H}$
$\quad OH = \dfrac{K_e}{H}$

885
$\quad FreetoTot = 1 + \dfrac{TS}{K_S}$
$\quad Hfree = \dfrac{H}{FreetoTot}$
$\quad HSO_4 = \dfrac{TS}{1 + \dfrac{K_S}{Hfree}}$
$\quad HF = \dfrac{TF}{1 + \dfrac{K_F}{Hfree}}$
$\quad Residual = TA - CAlk - BAlk - OH + Hfree + HSO_4 + HF$

890
$\quad Slope = DIC \cdot H \cdot K_1 \cdot (H^2 + K_1 \cdot K_2 + 4 \cdot H \cdot K_2)$
$\quad Slope = \dfrac{Slope}{Denom^2} + OH + H + \dfrac{BAlk \cdot H}{K_B + H}$
$\quad Slope = \log 10 \cdot Slope$
$\quad deltapH = Residual/Slope$! this is Newton's method
$\quad do\ while\ (abs(deltapH) > 1)\ deltapH = \dfrac{deltapH}{2}$! to keep the jump from being too big

895 $enddo$

$pH = pH + deltapH$! Is on the same scale as K$_1$ and K$_2$ were calculated, $i.e.$ total pH scale

$pCO_2 = \left(\dfrac{DIC \cdot H^2}{H^2 + K_1 \cdot H + K_1 \cdot K_2}\right) \cdot \dfrac{10^6}{K_0 \cdot FugFac}$! in µatm

$CO_2 = \dfrac{DIC \cdot 10^6}{1 + \dfrac{K_1}{H} + \dfrac{K_1 \cdot K_2}{H^2}}$

$HCO_3 = \dfrac{K_1 \cdot CO_2}{H}$

900 $CO_3 = \dfrac{K_2 \cdot HCO_3}{H}$

$Omega = \dfrac{Ca \cdot CO_3 \cdot 10^{-6}}{K_{ca}}$

Appendix B: Biogeochemical model variables and parameters

Table B1: Initial conditions of the state variables of Eco3M-CarbOx model (*diagnostic variables)

Variables	Name	Unit	values
Picophytoplankton	*PicoC*	mmolC m^{-3}	0.0480
	PicoN	mmolN m^{-3}	0.0092
	PicoP	mmolP m^{-3}	0.0003
Diatom	*DiaC*	mmolC m^{-3}	0.0571
	DiaN	mmolN m^{-3}	0.0089
	DiaP	mmolP m^{-3}	0.0007
Bacteria	*BacC*	mmolC m^{-3}	0.1083
	BacN	mmolN m^{-3}	0.0379
	BacP	mmolP m^{-3}	0.0039
DPOM **Detrital Particulate organic matter**	*DPOC*	mmolC m^{-3}	0.1252
	DPON	mmolN m^{-3}	0.0307
	DPOP	mmolP m^{-3}	0.0021
LDOM **Labile Dissolved organic matter**	*LDOC*	mmolC m^{-3}	1.0990
	LDON	mmolN m^{-3}	8.7980
	LDOP	mmolP m^{-3}	0.0018
DIM **Dissolved inorganic matter**	NH$_4$	mmolN m^{-3}	0.3375
	NO$_3$	mmolN m^{-3}	0.6723
	PO$_4$	mmolP m^{-3}	0.7150
	DO	mmolO m^{-3}	257.00
	DIC	μmolC kg^{-1}	2358.4
Total alkalinity	TA	μmolC kg^{-1}	2660.5
Sea water partial pressure of CO$_2$	*p*CO$_2$	μatm	371.28
***p*H**	*p*H	~~/~~	8.1099
calcium carbonate	CaCO$_3$	mmol m^{-3}	1.0000
Picophytoplankton chlorophyll	*PicoChl*	mgChl m^{-3}	0.0193
Diatom chlorophyll	*DiaChl*	mgChl m^{-3}	0.0229
Number of bacteria*	NBA	10^{12} cell m^{-3}	0.2000

905

Table B2: Balance equations of Eco3M-CarbOx model

Variables	Balance equation
Pico-phytoplankton	$\frac{\partial PicoC}{\partial t} = R_{PP}^{PicoC} - R_{resp}^{PicoC} - R_{exu}^{PicoC} - R_{Gr}$
	$\frac{\partial PicoN}{\partial t} = R_{uptPicoN}^{NH_4} + R_{uptPicoN}^{NO_3} - R_{exu}^{PicoN} - R_{Gr}$
	$\frac{\partial PicoP}{\partial t} = R_{uptPicoP}^{PO_4} - R_{exu}^{PicoP} - R_{Gr}$
	$PicoChl = Q_C^N \cdot \left(Q_{N,min}^{Chla} + f_Q \cdot \left(Q_{N,max}^{Chla} - Q_{N,min}^{Chla} \right) \right) \cdot PicoC$
Diatom	$\frac{\partial DiaC}{\partial t} = R_{PP}^{DiaC} - R_{resp}^{DiaC} - R_{exu}^{DiaC} - R_{Gr}$
	$\frac{\partial DiaN}{\partial t} = R_{uptDiaN}^{NH_4} + R_{uptDiaN}^{NO_3} - R_{exu}^{DiaN} - R_{Gr}$
	$\frac{\partial DiaP}{\partial t} = R_{uptDiaP}^{PO_4} - R_{exu}^{DiaP} - R_{Gr}$
	$DiaChl = Q_C^N \cdot \left(Q_{N,min}^{Chla} + f_Q \cdot \left(Q_{N,max}^{Chla} - Q_{N,min}^{Chla} \right) \right) \cdot DiaC$
Bacteria	$\frac{\partial BacC}{\partial t} = R_{uptBac}^{DPOC} + R_{uptBac}^{LDOC} - R_{BR} - R_{Gr}^{BacC}$
	$\frac{\partial BacN}{\partial t} = R_{uptBac}^{DPON} + R_{uptBac}^{LDON} + R_{uptBac}^{NH4} - R_{miner}^{NH4} - R_{Gr}^{BacN}$
	$\frac{\partial BacP}{\partial t} = R_{uptBac}^{DPOP} + R_{uptBac}^{LDOP} + R_{uptBac}^{PO4} - R_{miner}^{PO4} - R_{Gr}^{BacP}$
DPOM	$\frac{\partial DPOC}{\partial t} = R_{pf} + R_m - R_{Gr} - R_{uptBac}^{DPOC}$
	$\frac{\partial DPON}{\partial t} = R_{pf} + R_m - R_{Gr} - R_{uptBac}^{DPON}$
	$\frac{\partial DPOP}{\partial t} = R_{pf} + R_m - R_{Gr} - R_{uptBac}^{DPOP}$
LDOM	$\frac{\partial LDOC}{\partial t} = R_{exu}^{PicoC} + R_{exu}^{DiaC} + R_{exu}^{LDOC} - R_{uptBac}^{LDOC}$
	$\frac{\partial LDON}{\partial t} = R_{exu}^{PicoN} + R_{exu}^{DiaN} + R_{exu}^{LDON} - R_{uptBac}^{LDON}$
	$\frac{\partial LDOP}{\partial t} = R_{exu}^{PicoP} + R_{exu}^{DiaP} + R_{exu}^{LDOP} - R_{uptBac}^{LDOP}$
NH_4	$\frac{\partial NH_4}{\partial t} = R_{excr}^{NH_4} + R_{miner}^{NH_4} - R_{nit} - \sum R_{uptPhyN}^{NH_4} - R_{uptBac}^{NH_4}$
NO_3	$\frac{\partial NO_3}{\partial t} = R_{nit} - \sum R_{uptPhyN}^{NO_3}$
PO_4	$\frac{\partial PO_4}{\partial t} = R_{excr}^{PO_4} + R_{miner}^{PO_4} - \sum R_{uptPhyP}^{PO_4} - R_{uptBac}^{PO_4}$
DO	$\frac{\partial DO}{\partial t} = R_{aera} + \left(\frac{O}{C}\right) \cdot R_{PP}^{PhyC} + \left(\frac{O}{N}\right) \cdot R_{uptPhyN}^{NO_3} - \left(\frac{O}{C}\right) \cdot R_{resp}^{PhyC} - \left(\frac{O}{C}\right) \cdot R_{excr}^{DIC} - \left(\frac{O}{C}\right) \cdot R_{BR} - \left(\frac{O}{N}\right) \cdot R_{nit}$
DIC	$\frac{\partial DIC}{\partial t} = R_{aera} + R_{resp}^{PhyC} + R_{BR} + R_{excr}^{DIC} - R_{PP}^{PhyC} - R_{precip} + R_{diss}$
TA	$\frac{\partial TA}{\partial t} = 2 \cdot R_{diss} + \left(R_{uptPhyN}^{NO_3} + R_{uptPhyP}^{PO_4} - R_{uptPhyN}^{NH_4} \right) + R_{miner}^{NH_4} - 2 \cdot R_{precip} - 2 . R_{nit}$

Table B3: Biogeochemical processes simulated by the Eco3M-CarbOx model

Notation	Biogeochemical processes	Unit	Formulation	
R_{PP}^{Phy}	Primary production	molC m^{-3} s^{-1}	$R_{PP}^{PhyC} = P_{max} \cdot f_T^{PP} \cdot f_I \cdot PhyC$	$f_Q = min[f_Q^N, f_Q^P]; \; f_Q^X = \frac{Q_C^X - Q_{C,min}^X}{Q_C^X - Q_{C,min}^X + \beta_X}$ $f_T^{PP} = max\left(\frac{2 \cdot (1-b) \cdot \frac{(T-T_{let})}{(T_{opt}-T_{let})}}{\left(\frac{(T-T_{let})}{(T_{opt}-T_{let})}\right)^2 - 2 \cdot b \cdot \frac{(T-T_{let})}{(T_{opt}-T_{let})} + 1} ; 0\right)$ $f_I = \left[1 - exp\left(\frac{-\alpha_{Chla} \cdot E_{PAR} \cdot Q_C^{Chla}}{P_{max} \cdot f_Q \cdot f_T^{PP}}\right)\right]$
R_{resp}^{Phy}	Phytoplankton respiration	molC m^{-3} s^{-1}	$R_{resp}^{PhyC} = k_r^{PhyC} \cdot PhyC$	
$R_{uptPhy}^{NH_4}$	NH$_4$ uptake by phytoplankton	molX m^{-3} s^{-1}	$R_{uptPhyN}^{NH_4} = V_{N,max} \cdot \frac{NH_4}{NH_4 + K_{NH_4}}$	$V_{N,max} = Q_{C,max}^N \cdot R_{PP}^{Phy}$
$R_{uptPhy}^{NO_3}$	NO$_3$ uptake by phytoplankton	molN m^{-3} s^{-1}	$R_{uptPhyN}^{NO_3} = V_{N,max} \cdot \frac{NO_3}{NO_3 + K_{NO_3}} \cdot \left(1 - \frac{I_{in} \cdot NH_4}{NH_4 + K_{in}}\right)$	
$R_{uptPhy}^{PO_4}$	PO$_4$ uptake by phytoplankton	molP m^{-3} s^{-1}	$R_{uptPhyP}^{PO_4} = V_{P,max} \cdot \frac{PO_4}{PO_4 + K_{PO_4}} \cdot$	$V_{P,max} = Q_{C,max}^P \cdot R_{PP}^{Phy}$
R_{exu}^{PhyC}	Phytoplankton exudation as LDOC	molC m^{-3} s^{-1}	$R_{exu}^{PhyC} = (1 - f_Q) \cdot R_{PP}^{Phy}$	
R_{exr}^{PhyX}	Phytoplankton exudation as LDON or LDOP	molX m^{-3} s^{-1}	$R_{exu}^{PhyX} = (1 - h_Q^X) \cdot R_{uptX}^{Phy}$	$h_Q^X = \frac{Q_{C,max}^X - Q_C^X}{Q_{C,max}^X - Q_{C,min}^X}$
R_{BP}	Bacterial production	cell m^{-3} s^{-1}	$R_{BP} = \mu_{max}^{Ba} \cdot f_Q^{Ba} \cdot f_T^{Ba} \cdot NBA$	$f_T^{Ba} = Q_{10}^{\frac{(T-T_{rem})}{10}}$; $f_Q^{BA} = min\left[1 - \frac{Q_{C,min}^{BA}}{Q_C^{BA}}, 1 - \frac{Q_{N,min}^{BA}}{Q_N^{BA}}, 1 - \frac{Q_{P,min}^{BA}}{Q_P^{BA}}\right]$
R_{BR}	Bacterial respiration	molC m^{-3} s^{-1}	$R_{BR} = \rho_g^{Ba} \cdot \cancel{Q_C^{Ba} \cdot R_{BP}} \cdot Q_C^{Ba} \cdot R_{BP} + \rho_r^{Ba} \cdot \cancel{(Q_C^{Ba} - Q_{C,min}^{Ba})} \cdot (Q_C^{Ba} - Q_{C,min}^{Ba}) \cdot NBA$	
R_{uptBac}^X	X uptake by bacteria	molX m^{-3} s^{-1}	$R_{uptBac}^X = V_{max}^{BA} \cdot \frac{X}{X + K_X^{Ba}} \cdot f_T^{Ba} \cdot NBA$	
R_{Gr}^{Phy}	Phytoplankton grazing by zooplankton	molX m^{-3} s^{-1}	$R_{Gr}^{Phy} = g_{Phy} \cdot f_{Gr} \cdot Phy$	$f_{Gr} = \frac{Phy}{Phy + DPOM}$
R_{Gr}^{DPOM}	DPOM grazing by zooplankton	molX m^{-3} s^{-1}	$R_{Gr}^{DPOM} = g_{DPOM} \cdot f_{Gr} \cdot DPOM$	$g_{DPOM} = \frac{g_{Pico} \cdot Pico + g_{Dia} \cdot Dia}{Pico + Dia}$; $f_{Gr} = \frac{DPOM}{Phy + DPOM}$

R_{Gr}^{Bac}	Bacterial grazing by zooplankton	molX m^{-3} s^{-1}	$R_{Gr}^{Ba} = R_{BP} \cdot \frac{Bac}{NBA}$	
R_{excr}^{DIM}	Zooplankton excretion as DIC, NH$_4$ and PO$_4$	molX m^{-3} s^{-1}	$R_{excr}^{DIM} = \varepsilon_{DIM} \cdot d_X \cdot \left(1 - k_{X,zoo}\right) \cdot \left(R_{Gr}^{Phy} + R_{Gr}^{DPOM} + R_{Gr}^{Ba}\right)$	
R_{exu}^{LDOM}	Zooplankton exudation as LDOM	molX m^{-3} s^{-1}	$R_{exu}^{LDOM} = (1 - \varepsilon_{DIM}) \cdot d_X \cdot \left(1 - k_{X,zoo}\right) \cdot \left(R_{Gr}^{Phy} + R_{Gr}^{DPOM} + R_{Gr}^{Ba}\right)$	
R_{pf}	Zooplankton egestion	molX m^{-3} s^{-1}	$R_{pf} = (1 - d_X) \cdot \left(R_{Gr}^{Phy} + R_{Gr}^{DPOM} + R_{Gr}^{Ba}\right)$	
R_m	Zooplankton mortality	molX m^{-3} s^{-1}	$R_m = d_X \cdot k_{X,zoo} \cdot \left(R_{Gr}^{Phy} + R_{Gr}^{DPOM} + R_{Gr}^{Ba}\right)$	
R_{miner}	Mineralization of organic matter by bacteria	molX m^{-3} s^{-1}	$R_{miner}^X = \left(1 - h_Q^{Ba}\right) \cdot \left(R_{uptBac}^{LDOM} + R_{uptBac}^{DPOM} + R_{uptBac}^{DIM}\right)$	
R_{nit}	Nitrification	molX m^{-3} s^{-1}	$R_{nit} = k_{nit} \cdot f_T^{Ba} \cdot \frac{DO}{DO + K_{DO}} \cdot NH_4$	
R_{diss}	Carbonate dissolution	molC m^{-3} s^{-1}	$R_{diss} = (1 - \Omega_C) \cdot k_{diss} \cdot [CaCO_3]$	Ω_C = aragonite saturation
R_{precip}	Carbonate precipitation	molC m^{-3} s^{-1}	$R_{precip} = k_{precip} \cdot \frac{(\Omega_C - 1)}{K_C + (\Omega_C - 1)} \cdot \left(R_{PP}^{Phy} - R_{resp}^{Phy}\right)$	
R_{aera}	Gas exchange with atmosphere of DO or CO$_2$	molX m^{-3} s^{-1}	$R_{aera} = \frac{k_{ex}}{H} \cdot ([DO]_{sea} - [DO]_{sat})$ $R_{aera} = \frac{k_{ex}}{H} \cdot \alpha \cdot \left(pCO_{2,sea} - pCO_{2,atm}\right)$	$k_{ex} = 0.31 \cdot U_{10}^2 \cdot \frac{660^{0.5}}{Sc}$ H (depth), U_{10} (wind velocity) α (solubility), Sc (Schmidt number) and $[DO]_{sat}$ are function of T and S

Table B4: Value of parameters

Parameters		Pico	Dia	Unit	Reference
P_m^C	Maximal production	1.815	1.057	d^{-1}	Sarthou et al. (2005)
m_1	Fraction of the solar energy flux photosynthetically available	0.43	0.43	ǂ	Tett (1987)
m_2	Sea surface reflection	0.95	0.95	ǂ	Tett (1987)
m_3	More rapid attenuation of polychromatic light near the sea surface	1.0	1.0	ǂ	Tett (1987)
α_{Chla}	Chlorophyll-specific light absorption coefficient	8 10^{-6}	5 10^{-6}	m² molC (gChla J)$^{-1}$	Leblanc et al. (2018)
T_{opt}	Temperature optimal of growth	16.0	13.0	°C	ǂ
T_{let}	Lethal temperature	11.0	9.0	°C	ǂ
b	Shape factor for temperature curve	0.5	0.8	ǂ	Lacroix and Grégoire (2002)
β_N	Coefficient in the quota function	0.0072	0.002	molN molC^{-1}	Leblanc et al. (2018)
β_P	Coefficient in the quota function	0.0002	0.0005	molP molC^{-1}	Leblanc et al. (2018)
$Q_{C,min}^N$	Minimum phytoplankton N:C ratio	0.115	0.07	molN molC^{-1}	Leblanc et al. (2018)
$Q_{C,max}^N$	Maximum phytoplankton N:C ratio	0.229	0.18	molN molC^{-1}	Leblanc et al. (2018)
$Q_{C,min}^P$	Minimum phytoplankton P:C ratio	0.0015	0.006	molP molC^{-1}	Auger et al. (2011); Campbell et al. (2013)
$Q_{C,max}^P$	Maximum phytoplankton P:C ratio	0.0068	0.016	molP molC^{-1}	Auger et al. (2011); Campbell et al. (2013)
$Q_{N,min}^{Chla}$	Minimum phytoplankton Chl:N ratio	1.0	1.0	gChl molN^{-1}	Leblanc et al. (2018)**
$Q_{N,max}^{Chla}$	Maximum phytoplankton Chl:N ratio	2.2	2.7	gChl molN^{-1}	Leblanc et al. (2018)
k_r^{PhyC}	Phytoplankton respiration rate	0.099	0.099	d^{-1}	Faure et al. (2010)
K_{NO_3}	Half saturation constant for NO$_3$	0.73	1.0	mmolN m^{-3}	Leblanc et al. (2018)
K_{NH_4}	Half saturation constant for NH$_4$	0.07	0.015	mmolN m^{-3}	Leblanc et al. (2018)
K_{PO_4}	Half saturation constant for PO$_4$	0.008	0.01	mmolP m^{-3}	Leblanc et al. (2018)**
I_{in}	Factor of inhibition	0.82	0.82	ǂ	Harrison et al. (1996)
K_{in}	Amount of NH$_4$ from which assimilation by NO$_3$ is reduced.	0.578	0.578	mmolN m^{-3}	Harrison et al. (1996)
g	Grazing rate	1.452	0.846	d^{-1}	Gutiérrez-Rodríguez et al. (2011)

** calibrated from parameter used in the cited article

915 **Table B5: Value of parameters (continue)**

Parameters		Value	Unit	Reference
NBA	Number of bacteria	0.20	10^{12} cell m^{-3}	Moran (2015)
μ_{max}^{Ba}	Bacterial production rate	8.36	d^{-1}	Fraysse et al. (2013)
$Q_{C,min}^{BA}$	Minimum bacteria C:cell ratio	0.49	mmolC (10^{12} cell)$^{-1}$	Fukuda et al. (1998)
$Q_{N,min}^{BA}$	Minimum bacteria N:cell ratio	0.09	mmolN (10^{12} cell)$^{-1}$	Fukuda et al. (1998)
$Q_{N,max}^{BA}$	Maximum bacteria N:cell ratio	0.23	mmolN (10^{12} cell)$^{-1}$	Fukuda et al. (1998)
$Q_{P,min}^{BA}$	Minimum bacteria P:cell ratio	0.005	mmolP (10^{12} cell)$^{-1}$	Fraysse et al. (2013)
$Q_{P,max}^{BA}$	Maximum bacteria P:cell ratio	0.02	mmolP (10^{12} cell)$^{-1}$	Fraysse et al. (2013)
ρ_g^{Ba}	Factor of carbon respired by bacteria	0.60	⊥	Thingstad (1987)
ρ_r^{Ba}	Respiration rate of bacteria	0.01	d^{-1}	Thingstad (1987)
$V_{DPOC,max}^{BA}$	Maximum DPOC uptake by bacteria	0.029	mmolC (10^{12}cell10^{12} cell)$^{-1}$ d^{-1}	Campbell et al. (2013)
$V_{LDOC,max}^{BA}$	Maximum LDOC uptake by bacteria	16.33	mmolC (10^{12} cell)$^{-1}$ d^{-1}	Campbell et al. (2013)
$V_{DPON,max}^{BA}$	Maximum DPON uptake by bacteria	0.05	mmolN (10^{12} cell)$^{-1}$ d^{-1}	Faure et al. (2010)
$V_{LDON,max}^{BA}$	Maximum LDON uptake by bacteria	0.32	mmolN (10^{12} cell)$^{-1}$ d^{-1}	Faure et al. (2010)
$V_{NH_4,max}^{BA}$	Maximum NH$_4$ uptake by bacteria	0.32	mmolN (10^{12} cell)$^{-1}$ d^{-1}	Faure et al. (2010)
$V_{DPOP,max}^{BA}$	Maximum DPOP uptake by bacteria	0.01	mmolP (10^{12} cell)$^{-1}$ d^{-1}	Thingstad (1987)
$V_{LDOP,max}^{BA}$	Maximum LDOP uptake by bacteria	0.48	mmolP (10^{12} cell)$^{-1}$ d^{-1}	Thingstad (1987)
$V_{PO_4,max}^{BA}$	Maximum PO$_4$ uptake by bacteria	0.48	mmolP (10^{12} cell)$^{-1}$ d^{-1}	Thingstad (1987)
K_{DPOC}^{BA}	Half-saturation constant for DPOC	10.0	mmolC m^{-3}	Faure et al. (2010)
K_{LDOC}^{BA}	Half-saturation constant for LDOC	25.0	mmolC m^{-3}	⊥
K_{DPON}^{BA}	Half-saturation constant for DPON	0.50	mmolN m^{-3}	⊥
K_{LDON}^{BA}	Half-saturation constant for LDON	0.50	mmolN m^{-3}	⊥
$K_{NH_4}^{BA}$	Half-saturation constant for NH$_4$	0.15	mmolN m^{-3}	Leblanc et al. (2018)
K_{DPOP}^{BA}	Half-saturation constant for DPOP	0.08	mmolP m^{-3}	⊥
K_{LDOP}^{BA}	Half-saturation constant for LDOP	0.08	mmolP m^{-3}	Leblanc et al. (2018)
$K_{PO_4}^{BA}$	Half-saturation constant for PO$_4$	0.02	mmolP m^{-3}	Campbell et al. (2013)
ε_{DIC}	fraction excretion of DIC	0.31	⊥	Faure et al. (2010)
ε_{NH_4}	fraction excretion of NH$_4$	0.50	⊥	Faure et al. (2010)
ε_{PO_4}	Fraction excretion of PO$_4$	0.50	⊥	Fraysse et al. (2013)
d_C	Fraction of C assimilated	0.92	⊥	Gerber and Gerber (1979)
d_N	Fraction of N assimilated	0.95	⊥	Faure et al. (2010)
d_P	Fraction of P assimilated	0.95	⊥	Fraysse et al. (2013)
$k_{C,zoo}$	Net C growth efficiency	0.40	⊥	Gerber and Gerber (1979)
$k_{N,zoo}$	Net N growth efficiency	0.44	⊥	Le Borgne and Rodier (1997)
$k_{P,zoo}$	Net P growth efficiency	0.37	⊥	Le Borgne (1982)
Q_{10}	Temperature coefficient	2.0	⊥	⊥
T_{rem}	Reference temperature for mineralization	20.0	°C	⊥
k_{nit}	Nitrification rate	0.05	d^{-1}	Lacroix and Grégoire (2002)
T_{nit}	Reference temperature for nitrification	10.0	°C	⊥

Tableau mis en forme

Tableau mis en forme

Mis en forme : Centré

Mis en forme : Centré

Mis en forme : Centré

37

37

K_{DO}	Half-saturation constant DO	30.0	$mmolO_2\ m^{-3}$	Tett (1990)
k_{diss}	Dissolution rate	10.9	d^{-1}	Gehlen et al. (2007)
k_{precip}	Fraction of PIC to LPOC	0.02	-	Marty et al. (2002)
K_C	Half-saturation constant of $CaCO_3$ precipitation	0.40	$(\mu mol\ kg^{-1})^2$	
$\left(\dfrac{O}{C}\right)$	Ratio O:C	1.0	-	-
$\left(\dfrac{O}{N}\right)$	Ratio O:N	2.0	-	-

Mis en forme : Centré

Mis en forme : Centré

Appendix C: Short User Manual

After uploading the whole archive on the zenodo site (ref. doi: 10.5281/zenodo.3757677), the exact version of the Eco3M-CarbOx
920   code used in this study can be ~~be~~ run as following:

make !two executable files will be created : eco3M_ini.exe and eco3M.exe

- the file config.ini allows to define: the time, time step, and save time of simulation variables biogeochemical process
- Results files are stocked in "SORTIES" directory
- Boundary conditions and forcings data are stocked in "DATA" directory
925 - All subroutines of biogeochemical processes are stocked in "F_PROCESS" directory

For further information, please contact Dr. Frédéric DIAZ (frederic.diaz@univ-amu.fr) or Dr. Christel PINAZO (christel.pinazo@univ-amu.fr)

930 "Implementation and assessment of a carbonate system model (Eco3M-CarbOxv1.1) in a highly-dynamic Mediterranean coastal site

(Bay of Marseille, France)"

submitted for publication to Geoscientific Model Development

by K. Lajaunie-Salla and co-authors

935

General reply: We thank again the Reviewer Dr Munhoven for his second evaluation of our work. We thank too him for the detailed and useful comments that contributed to greatly improve the manuscript. We consider all of his comments to improve the manuscript.

940

1. General comments

The authors' reply the revised manuscript are not very "reviewer-friendly." It is nowadays standard practice to provide a "track change" (or a LATEXDIFF) version of the manuscript clearly identifying the changes made to the text, right in the text. The equivalent information is seemingly given in the reply, except that the line numbers provided there do not match, so that one has to search

945 manually for the exact location of the changes.

The preparation of the manuscript would also have benefited from some extra care. Page numbers restart at 1 after page 23 without any apparent reason.

Reply: The preparation of the revised ms has been reviewed with care and page numbers have been reprocessed. A new check of the different sections has been carefully performed.

950

1.1 Appreciation of the replies to reviewers

The authors have all in all well responded to the referees' comments, with one exception though. In the response to my comment 2.3, regarding the missing effect of river intrusions on DIC — TA perturbations are taken into account, but as these are carried mainly by HCO_3^- , they also generate DIC perturbations of the same magnitude, which are neglected — I read at the top of the fourth page (page

955 numbers in the response would have been helpful) that

"Concerning the riverine inputs scenarii, we decide to focus on nitrate and alkalinity supply. In fact the model simulates the DIC increases, as is observed, which highlight that the carbonate system module is well resolved."

The reply to the comments is somewhat ambiguous as suggests that DIC changes are taken into account, while they are actually not, as stated in the manuscript at lines 413–414 :

960 " [. . .] the experimental design on the Rhône River supply only considers the TA perturbation on the carbonate system but not that due to the DIC supply."

So, even if the model reproduces the observed DIC increases (as stated in the reply), this must obviously be for the wrong reasons, as only one half of the effects of the perturbation due to river intrusions is taken into account. By the way, no one argued that the carbonate system module was not well resolved.

965 *Reply: We decided to remove the scenario of AT supply by river and all the text referred to it in the methods and results/discussion sections. See our detailed comment on this point hereafter.*

1.2 Appreciation of the revised manuscript

The model description has been improved and the rationale behind the carbonate speciation calculations is now presented in a new

970 appendix. Unfortunately, the layout of that appendix is rather chaotic which makes it difficult to read.

2. Specific comments

2.1 River intrusion experiments: poor justification

The justification added at lines 414–417 for taking the effect of river intrusions into account only in terms of the resulting TA but not DIC perturbations is rather cavalier and scientifically untenable. This is a completely unrealistic assumption that makes the outcome of the experiment meaningless and thus essentially invalidates any conclusion drawn from it.

I only see two options to address this shortcoming:

1. the river intrusion experiments are repeated with the effect on DIC included (which should be rather straightforward to correct) and the discussion of the results adapted;

2. these experiments are simply taken out of the paper as the current results are essentially unfounded.

Even in preliminary experiments, one must not choose to disregard one of two effects of a perturbation if these are of the same order of magnitude. Such arbitrary choices lead to arbitrary results.

Reply: We have chosen the second option proposed by the Reviewer. Mainly because it was not straightforward to consider DIC supply by River as considered for AT. In fact, DIC is not as conservative as AT is regard to salinity. It is then impossible to use a relationship between DIC and salinity as that used between AT and salinity in the previous version of our manuscript. In the context of a 0D modelling developed here, this kind of relationship would have been the only mean to take into account the DIC supply by the Rhône River. In the revised version, we stressed (l 398-401) that rivers also supply TA and DIC and a consideration for these supplies in future works may sensibly modify the modeled carbonate balance in the BoM compared to that presented in this study. Concomitantly we slightly rewrote the end of section 4.1 on the model performance in Discussion.

As noted in the conclusion (l434), a coupling of the Eco3M-CarbOx model to a 3D hydrodynamics model is planned to better represent the complexity of functioning of the BOM. This implementation will enable, for example, to take into account actual DIC and AT supplies from the Rhône River by considering forcing values measured in the River.

3. Technical comments

Reply: All these technical comments have been taken into account in the new revised version of ms.

Page 1, line 22: "the year 2017 that is a period for which" should read "the year 2017 for which"

Page 1, line 25: "of most of variables of carbonate system except Total Alkalinity." should read "of most of the variables of the carbonate system except for Total Alkalinity."

Page 1, line 26: "experiments were also conducted" should read "experiments were conducted"

Page 1, line 26: "to (i) seawater" should read "to (i) a seawater"

Page 1, line 27: "Rhône River plume intrusion" should read "Rhône River plume intrusions"; by the way: the name of that river is sometimes spelled "Rhône", more often "Rhone" — please use the same spelling consistently throughout

Page 1, line 35: "external forcing have" should read "external forcings have"

Page 5, line 188: "a salinity threshold of 37 has been chosen" – is this correct? A threshold of 37 looks rather high to me.

Page 6, line 226: "during MWC period" should read "during the MWC period"

Page 7, line 271: "15 March and 6 May" should either read "15th March and 6th May" or "March 15th and May 6th" (as on line 277, p. 8)

Page 11, line 390: "Moreover, previous study" should read "Moreover, a previous study", or even better reformulate the sentence to read "Moreover, Fraysse et al. (2013) highlight that . . . " and discard the citation in brackets.

Page 11, line 402: "a longer period ca. 15 days" should read "a longer period of ca. 15 days"

Page 11, lines 402–403: "high atmospheric pCO2 value and wind speed" better had to read "high atmospheric pCO2 and high wind speeds"

1015 Page 11, line 411: "due to some two" should read "due to two"

29th and 30th pages (pages nr. 6 and 7), throughout: "in the pH scale" should read "on the pH scale"

29th page (page nr. 6): "Concentration in Total Fluoride (TF) ions" should read "Total Fluoride concentration" (without "ions," as TF includes the non ionic HF)

29th page (page nr. 6): "Concentration in Total Sulphate (TS) ions" should read "Total Sulphate concentration" ("ions" is superfluous)

1020 29th page (page nr. 6): "Concentration in Total Boron (TB)" should read "total boron concentration" (without "ions," as TB includes the non ionic B(OH)3)

29th page (page nr. 6): KF is the dissociation constant of hydrogen fluoride (or of hydrofluoric acid), not of fluoride ions

29th page (page nr. 6): in the expression for KF, the exponent for Ions should be 0.5 (or 1/2) and not 1.5.

30th page (page nr. 7): "Every constant are corrected by the hydrostatic pressure" should read "All the constants are corrected for the

1025 effect of hydrostatic pressure"

Guy Munhoven
Liège, 9th October 2020

1030

42